Review of Literature

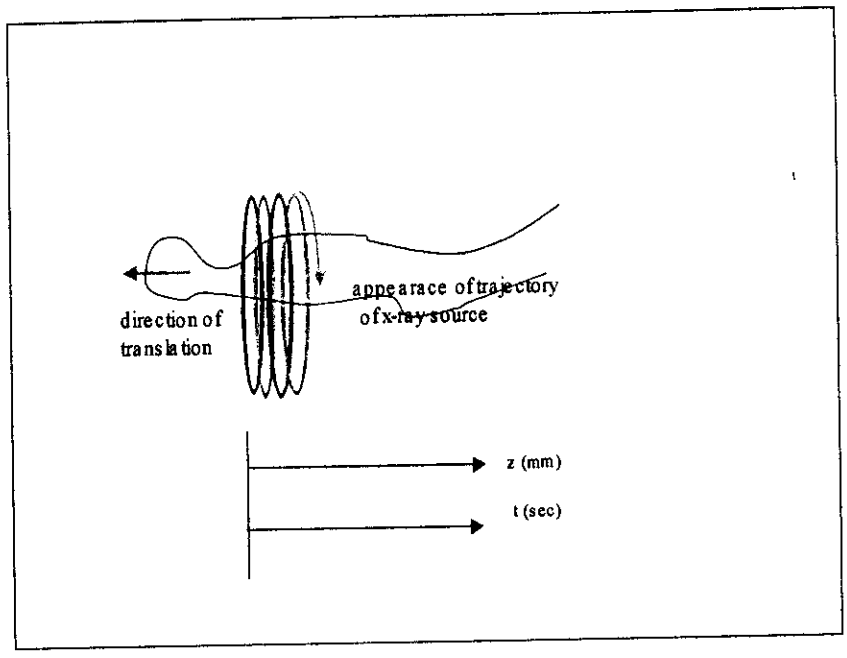

Fig.1

Spiral CT data acquisition geometry translation of the patient in the direction shown is equivalent to translation of the scanner in the opposite direction. The apparent trajectory of the x-ray source is a spiral or helix surrounding the patient. The projection of the source as a function of time onto the scanner axis (z-axis) is a line segment that begins at the position from which the patient begins to move and whose end point travels at the same speed as the patient, but in the opposite direction.(After Napel, 1998).

THORACIC APPLICATION OF SPIRAL CT

Spiral CT has revolutionized the way in which chest disorders are evaluated. With spiral CT, continuous table feed and synchronous data acquisition generate a volumetric acquisition that can be performed during a single breath-hold **(fig 1) (Vock et al, 1990; Kalender et al, 1990; Costello, 1994).**

Limitations of conventional CT for chest imaging

The traditional stepwise technique with interscan delays of 3-10 sec between axial slices often results in slice misregistration because of variations in depth of inspiration from one CT slice acquisition to the next. Slice misregistration, patient motion, and partial volume averaging with conventional CT increase the likelihood of missing significant pathology in the lung **(Costello, 1994).**

Advantages of spiral CT for chest imaging

Spiral CT is essentially a gapless scanning technique. Volume acquisition eliminates discontinuities between slices. Spiral CT performed during a single breath-hold further limits respiratory motion **(Vock et al, 1990; Kalender et al, 1990).** The resulting data set allows the generation of superior multiplanar and 3-D images. An added benefit of spiral CT is that the faster scanning times eliminate delays during IV injection, allowing for superior vascular enhancement with smaller amounts of IV contrast **(Kalender et al, 1990; Costello, 1994; Zeman et al, 1995).**

Spiral technique

Spiral CT options of chest imaging

The optimal, single best spiral CT protocol for imaging the chest has yet to be determined. When performing spiral CT examination of the chest, the radiologist has a number of new parameters to manipulate compared to conventional CT scanning, including linear interpolation algorithm, reconstruction algorithms, slice

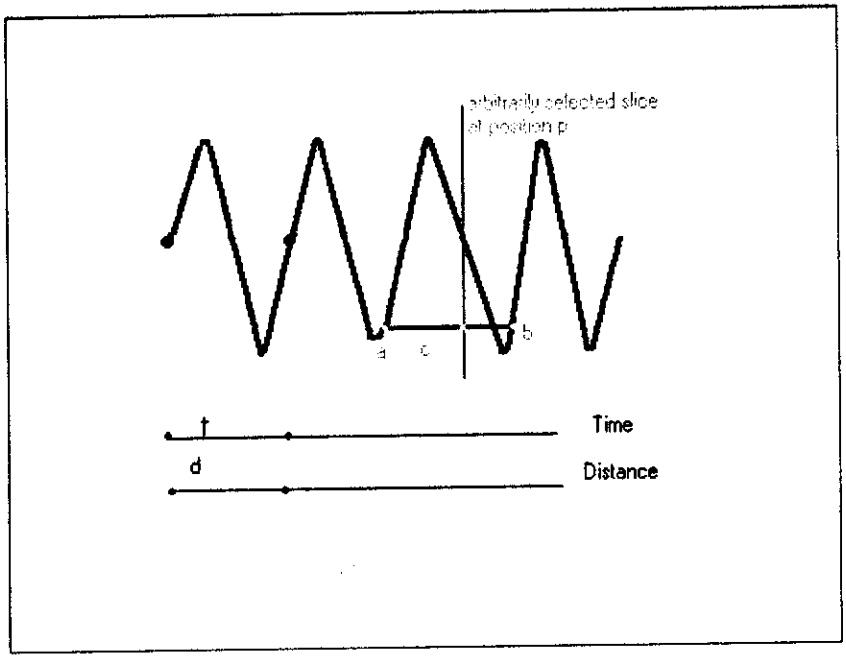

Fig.2

Graph illustrates principle of linear interpolation, which refers to a mathematical technique of deriving data at a given point from two adjacent data points. Data at point c on an arbitrarily selected plane p is derived by linear interpolation between points a and b. Data points a and b are two points nearest to point c at same degree of rotation (for 360° linear interpolation). t = time required for one gantry rotation (360°), d= distance traveled by table in one gantry rotation (360°). (After Paranjpe and Bergin, 1994).

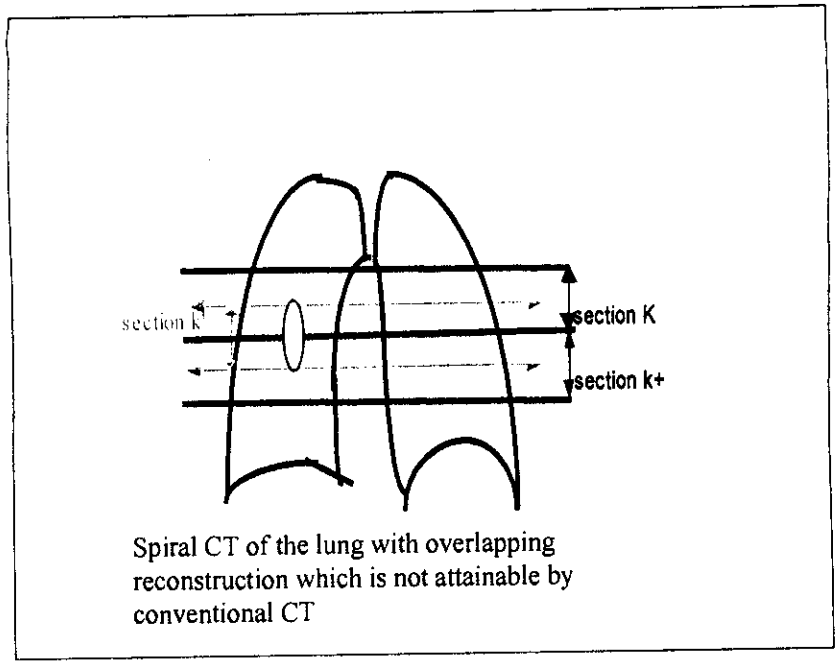

Fig.3

Illustration of intensity loss due to through-plane partial volume effect. The full width at half maximum of the SSP is given by the separation between solid lines. The lesion is only partly imaged by section K and K+1; thus its intensity will be decreased due to volume averaging with surrounding soft tissue . However, section K', which can be positioned and reconstructed from the acquired spiral projection data, images the lesion with less volume averaging with greater intensity.(After Napel, 1998).

acquisition thickness, slice reconstruction interval, table speed, duration of scan, and single versus variable mode of acquisition.

By optimizing each of these parameters, the CT radiologist can customize a spiral CT examination by taking into account patient and equipment factors as well as the particulars of the chest problem to be investigated **(Janet, 1998)**.

1-Linear interpolation algorithms

Image generation in spiral CT is accomplished through a process of linear interpolation that reconstructs planar images from the raw spiral data **(fig 2)**. The first generation of spiral CT scanners used a 360-degree linear interpolation algorithm. These older algorithms have now replaced by newer, improved 180-degree linear interpolation algorithms that result in less broadening of the section sensitivity profile and less blurring of the images **(Polacin et al, 1992).**

2-Reconstruction Algorithms

Depending on the manufacturer, a number of image display reconstruction algorithms are also available. A standard or soft tissue algorithm is usually chosen for display of soft tissue structures of the mediastinum and chest wall, where as a lung algorithm is preferable for displaying the lung parenchyma. Newer high-resolution lung algorithms available on some manufacturer's scanners dramatically improve image quality for lung detail **(Janet, 1998)**.

3-Reconstruction interval

The interval at which each planar CT image is reconstructed (the degree of overlap between reconstructed axial images and the reconstruction incrementation) is a new spiral CT parameter that must be designated by the operator. For example, each 10-mm thick slice may be reconstructed every 10-mm with no overlap or every 5 mm, giving an overlap of 5 mm. As a general rule when performing chest studies, reconstructing images at an interval that is one-half the slice thickness (two images per slice incrementation) increases the information gained from the spiral CT data set **(fig 3)**. Little additional information is gained by reconstructing

at close intervals, unless one is performing CT angiography or multidimensional imaging **(Janet, 1998)**.

Reconstructing images at closer intervals increases the number of images that must be filmed and reviewed, increasing both the dollar and time cost of the examination **(Brink, et al 1994).**

4-KVp, mA, Duration of spiral scan, Scanning mode

Specific spiral CT scanning parameters, such as Kilovolt peak (KVp) and milliampere (mA) settings, vary by manufacturer and should be adjusted for patient characteristics.

The maximum spiral imaging time for one spiral acquisition or the duration of the scan depends on the manufacturer's available x-ray power and the patient's ability to hold his or her breath **(Brink et al, 1994).** The option to perform only a single spiral CT acquisition versus multiple spiral acquisitions in rapid succession–so–called variable-mode spiral CT– also varies among manufacturers. In variable-mode spiral CT, a series of shorter spiral CT acquisitions can be preprogrammed to be acquired sequentially with short breaks between the acquisitions to allow the patient to breathe **(Brink et al, 1994; Tomiak et al, 1995; Foley & Oneson, 1994; Korobkin 1994).** This mode of scanning is preferable for patients who cannot hold their breath for the extended 24-40 sec required for a single acquisition spiral scan. It is also ideal for combined chest and abdomen studies that use a single injection of IV contrast, as is often employed when scanning cancer patients for lung and liver metastases. Variable-mode spiral CT allows both the pulmonary hila and the liver to be imaged during their optimal phases of the contrast enhancement **(Foley& Oneson, 1994; Korobkin, 1994).**

5-Slice Acquisition Thickness and Table speed

Slice acquisition thickness or beam collimation can be varied from 1 to 10-mm in thickness in most spiral CT scanners. Table speed can also be varied from 1 to 10-mm/sec. Choice of slice thickness and table speed depends on the clinical question of concern and determines the pitch that is used.

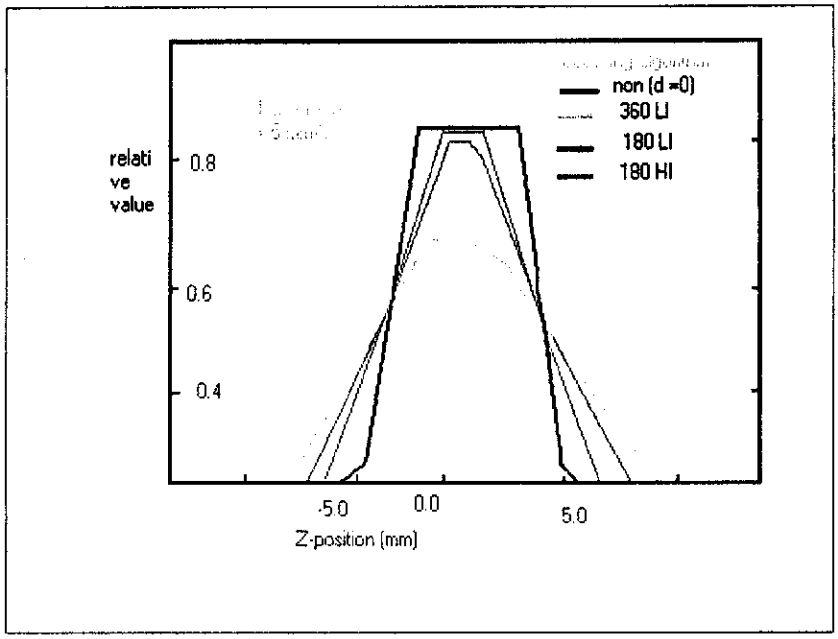

Fig.4

Section sensitivity profiles for different spiral CT algorithms (5-mm collimation, pitch of 1). The profiles for the 180° interpolation nearly approximate that of the rectangularly shaped profile of conventional scanning. 360 LI = 360° linear interpolation, 180 LI = 180° linear interpolation, 180 HI = 180 ° higher-order (cubic spline) interpolation, d = table feed (mm/s), Z-position = longitudinal position (mm).(From Brink, 1995).

Pitch

Pitch is defined as the "table feed distance per 360-degree tube rotation divided by the nominal section thickness". Because each 360-degree rotation occurs in 1 sec, Pitch = Table speed / Slice thickness.

Using a pitch of 1 is generally a good compromise in the chest to achieve adequate area coverage with a minimum of *z*-axis blurring. A pitch of more than 1 is valuable if a larger volume needs to be covered in a single breath-hold acquisition **(Brink et al, 1994).** Increasing the pitch widens the section sensitivity profile, which in turn causes increased partial volume averaging and *z*-axis blurring. The impact of the image quality is lessened to certain extent in the chest, where there is high inherent contrast between structures. Widening of the section sensitivity profile has also been markedly decreased by the newer 180-degree interpolation algorithms on modern spiral scanners **(Wright et al, 1996).** In the chest, pitches of 1.5-1.7 can be used with little apparent degradation of image quality caused by *z*-axis blurring **(fig 4)**.

By choosing a pitch of more than 1 and decreasing the slice collimation, the same volume of tissue can be scanned in the same time with higher spatial resolution **(Rubin & Napel 1995).** For example, by increasing the pitch to 1.7 and decreasing slice thickness from 10-mm to 6 mm, one can actually improve the spatial resolution within the axial plane but still cover the same territory in the chest in the same amount of time. However, decreasing slice collimation increases pixel noise **(Brink et al, 1994; Rubin & Napel 1995).**

Wright et al. studied the effect of increasing the pitch on pulmonary nodule detection and found a tendency to undercount lung nodules as pitch increased above 1.5. Spiral artifacts also become more noticeable at higher pitches. One such artifact consists of an area of an image dropout or low attenuation that occurs at branch points of vessels at pitches of more than 1.5**(Wright et al, 1996).**

The trade-off in the chest can be summarized as follows: increasing pitch allows the use of thinner-slice collimation with resultant higher spatial resolution and

lower radiation dose, but at the expense of increased pixel noise and more noticeable spiral CT artifacts (**Brink et al, 1994; Wright et al, 1996; Rubin & Napel 1995**). Understanding these trade-offs allows one to choose the slice thickness and pitch that are most appropriate for the individual examination.

Optimizing spiral CT technique for the chest

Two protocols have been found practical for most chest imaging.

For studies of the chest requiring fine detail and high resolution but a limited area of coverage, the following parameters are preferred: 3-5 mm section acquisition thickness, table speed of 3-5 mm /sec, pitch 1, high resolution algorithm (lung algorithm on GE system), and reconstruction of overlapping slices every 1-2 mm. The distance covered can be increased by increasing the pitch from 1 to 1.5-1.7 (**Janet, 1998**).

The second protocol is used when the entire chest must be covered in a routine fashion (e.g., as a screening or follow up examination for pulmonary pathology). Using 10-mm slice acquisition thickness, 10-mm /sec table speed, pitch 1, lung algorithm, and reconstruction of overlapping slices every 5-mm. The use of a 50% overlap of reconstructed images is particularly useful when screening or following lung metastases.

Using a variable-mode acquisition, a series of 3 or 4 back-to-back, 7-10-sec helical scans is often chosen for patients who find it difficult to hold their breath for an extended period of time. If it is more desirable to scan the entire chest during a single breath-hold (e.g., to generate multiplanar or 3-D images of the airways or vessels), a single 30-32-sec spiral acquisition is chosen, pitch is increased from 1 to 1.5-1.7, and the narrowest slice collimation that will cover the distance required in the chest is chosen (usually 5-7 mm). The images can then be reconstructed at 2-3 mm intervals.

Also it is helpful to hyperventilate the patient by having him take 3 deep breaths just before the spiral scan. After taking the 3 breaths in and out, the patient is then

asked to take in a deep breath and hold it. With this type of preparation, many patients can successfully hold their breath for 24-32 sec (**Janet, 1998**).

Peridiaphragmatic pathology

Evaluation of peridiaphragmatic nodules and processes is particularly difficult with conventional CT because of the degree of excursion of the lung bases and diaphragm from one breath to the next tends to be great (estimated to be up to 8 cm) and quite variable (**Costello, 1994; Brink et al, 1994**).

Spiral CT acquired during a single breath-hold maneuver eliminates problems with respiratory excursions and facilitates examination of nodules and abnormalities near the diaphragm. Additional information regarding the relationship of the lesion and the diaphragm can be gained from multiplanar images in the coronal and sagittal plane that are free of the respiratory artifacts (**Costello, 1994**).

2 / 3 D imaging of the thorax

With the advent of spiral CT, high-quality multiplanar and 3D images of the lung are now possible.

The improved quality of the reconstructed images is due to the fact that spiral CT is volume acquisition obtained during a single breath-hold. This eliminates interslice variability and discontinuities between slices that degrade reformatted images.

A number of 3D techniques can be applied to spiral CT data sets, including thresholding and surface-rendering techniques, maximal- or minimal-intensity projections and volumetric rendering (**Zeman et al, 1995**). The advantage of 2 D and 3 D imaging of spiral CT data are numerous. It allows for multiplanar and 3 D display of the airways and pulmonary vasculature, enabling the bronchoscopist or surgeon to obtain a through understanding of the anatomy and pathology prior to procedures. In addition, the volume of a given region of interest can be measured in three dimensions.

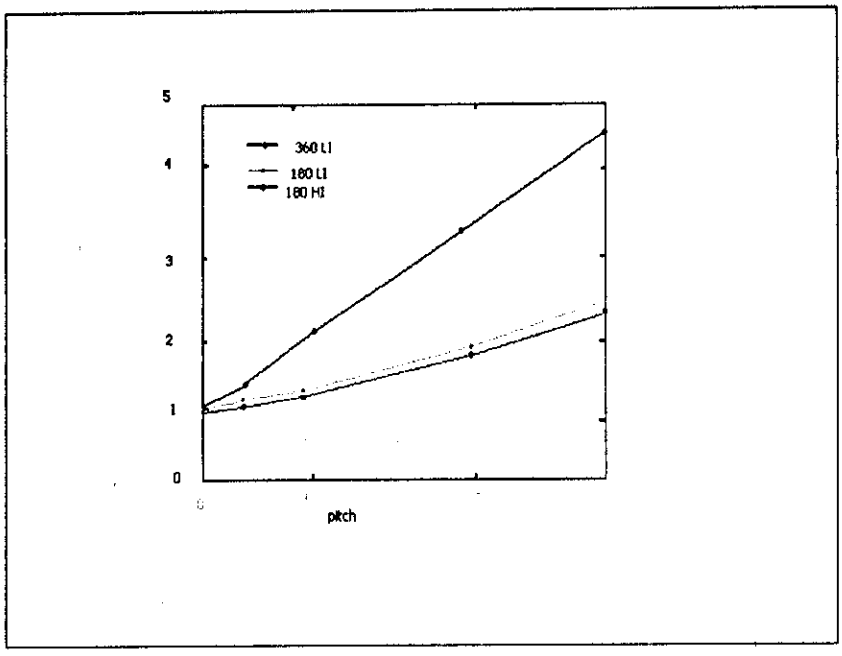

Fig.5

Slice thickness versus pitch for three different interpolation algorithms. A substantial improvement in slice thickness broadening is seen with 180 ° interpolation (180 LI, 180 HI) for pitch >1 as compared to 360 ° interpolation (360LI). Graph displays simulated slice thickness (defined here as the full width at tenth maximum of the section sensitivity profile) for spiral CT performed with 5-mm collimation. Pitch = 0 refers to conventional scanning, 360LI = 360 ° linear interpolation, 180LI =180 ° linear interpolation, and 180 HI = 180 ° higher-order (cubic spline) interpolation. (From Brink, 1995)

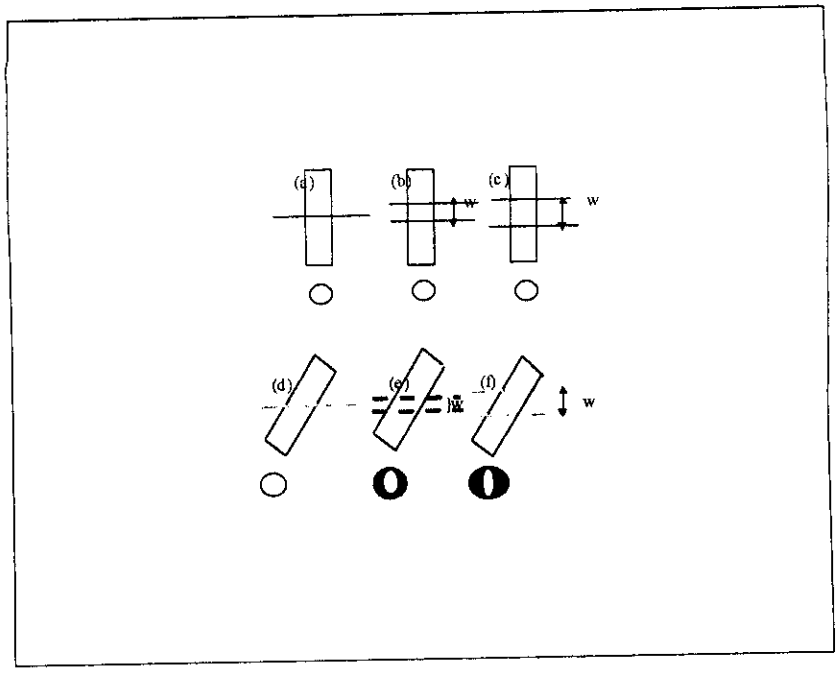

Fig.6

Illustration of perceived loss of in-plane spatial resolution with increasing section thickness. Each subfigure shows a coronal view of a cylinder (solid line) and a measure of the section thickness w for the axial view below (ellipse).

(a) Cylinder is aligned perpendicular to a thin-section plane. Axial image is a sharply defined circle.

(b,c) Axial image is unchanged when scanned with thicker sections.

(d) Cylinder; is inclined with respect with section plane. For the thin-section plane, the axial image is a sharply defined ellipse.

(e,f) As the section becomes thicker, the edges of the ellipse are less sharply resolved due to partial volume. The result is that the ellipse appears less sharp with increasing section thickness.(After Napel, 1998)

A future application of 2D /3D spiral CT may be in oncology, to generate sophisticated 3D tumor volumetrics for planning and assessing tumor response to chemotherapy and radiation therapy **(Kuriyama et al, 1994).**

Disadvantage and limitations

Because of heat build up in the x-ray tube, there are limits in the amount of milliamps that can be generated over an extended period of time during a spiral CT acquisition. Depending on the manufacturer, there are also some postprocessing delays that occur while the spiral CT images are being reconstructed. Computer and data storage capacities on many scanners do not allow for unreconstructed data to be stored indefinitely.

The nature of the spiral CT data acquisition process and reconstruction algorithm creates certain unique problems **(Kalender, 1995).** When compared with conventional CT, spiral CT shows broadening of the section sensitivity profile, demonstrating a greater full width at half maximum (FWHM =1.8 for spiral CT using 360-degree-LI)**(Kalender et al 1990)**. Broadening of the slice thickness is due to table transport during the spiral CT scan. This results in *Z*-axis blurring or blurring along the longitudinal table axis. *Z*-axis blur manifests itself on spiral CT images as lack of sharpness due to increased volume averaging **(fig 5)**. It is particularly noticeable for structures oriented obliquely to the *Z*-axis or structures whose cross-sectional diameter changes rapidly along the table feed direction **(fig 6)(Polacin et al, 1992; Kalender & Polacin 1991)**. *Z*-axis blur can be minimized by decreasing the speed of table feed with respect to the beam collimation (i.e., decreasing the pitch) and by narrowing the beam collimation with greater overlap of reconstructed images **(Kalender, 1995; Kalender et al, 1994; Wang & Vannier 1994).** Using a high-resolution or sharp algorithm also seems to help. Newer 180-degree interpolation algorithms also significantly decrease the amount of *Z*-axis blur and demonstrate section-sensitivity profiles with FWHM as low as 1.1 **(Polacin et al, 1992; Brink et al, 1994).**

Trade-offs for spiral CT are between (a) increasing speed, greater distance covered, and lower radiation dose, and (b) increasing *Z*-axis blur and artifacts. For example, if a large area of interest needs to be scanned, one must choose a faster table speed and perhaps greater pitch, but at the cost of increased *Z*-axis blurring. Another trade-off is between increasing spiral scan time and maximum milliamps allowed. For longer scan times of 32-40 sec, only a lower maximum milliamperage is possible on many scanners. This will increase pixel noise and may be noticeable when examining large patients (**Janet, 1998**).

HRCT versus Spiral CT

Spiral CT has replaced conventional CT technique. If one compares a high-resolution CT with 1-mm thick collimation to a spiral CT, the differences in resolution are clearly visible.

Spatial resolution and linear edge detection are superior with HRCT techniques. Although linear structures are delineated better with HRCT, small nodules are better demonstrated with spiral CT **(Zeman et al, 1995).**

One approach that combines the advantages of both techniques is to start examination with a survey study of the chest using spiral CT technique and follow that with a few select HRCT images as needed **(Janet, 1998)**.

Radiation dose of the patient from a spiral CT

Because spiral CT employs continuous scanning, the x-ray-tube power (i.e., the highest permissible milliampere-second setting) is currently limited to less than that used for standard CT scanning. This power limitation is greatest for long scans (e.g., 24 seconds or longer) and results in increased quantum noise. Given the same x-ray-tube power, the radiation dose to the patient for a spiral CT scan is equal to that for standard continuous-section CT, if a pitch is 1 is used (i.e., if table speed is matched to the collimation). Radiation dose for a spiral CT is decreased when the pitch is greater than 1, compared with standard continuous-section CT. Since the highest permissible milliampere-second setting for long-duration spiral scans is currently less than that used for standard CT, the radiation dose to the

patient is currently less for long duration spiral CT **(Heiken et al, 1993)**. In addition, the need to rescan areas of interest is much less common with spiral CT than with conventional CT. This particularly true for chest examinations when evaluating a small, solitary pulmonary nodule. **(Janet, 1998)**

Subsecond Spiral CT scanning

Spiral CT continues to evolve with each new scanner introduced providing, specific and unique features designed to either optimize classic scanning protocols or to develop newer study protocols or even completely new application.
Total length of single spiral CT acquisitions has increased from 20-24 sec range in 1993 to 40-50 sec range in 1998. Similarly, initial scan parameters included values in the 140-210 mA range, where current systems provide values in the 280-320 mA range, making spiral protocols similar to standard dynamic CT protocol parameters. The most recent advance has been the introduction of subsecond spiral CT scanning. Classically, spiral CT scanners complete a single 360-degree scanner rotation in 1 sec, which means that the gantry rotates at a rate of 60 revolutions per minute (rpm). Introduction of advanced scanner technology permits the gantry to rotate at 80 rpm, so that 360-degrees are traversed in 0.75 sec. This means that 1.33 rotations/sec are achieved, with the rotation speed 33% faster. Thus when using subsecond spiral CT, a 33% larger volume can be acquired with identical resolution and pitch. For example, a pitch of 1 and 10-mm collimation set for 1-sec spiral CT scan will travel 10-mm/sec, where as at 0.75 sec with the same pitch and collimation setting will travel 13.33 mm/sec. With 0.75-sec scanner, a larger distance can be covered with similar collimation **(Fishman, 1997).**

Spiral CT of parenchymal lung disease

Over the past decade, thin-section CT has been widely performed to evaluate patients with diffuse infiltrative lung disease (DILD). By the direct visualization of fine details within the lung, such as septal and polygonal lines, honeycombing, and

traction bronchiectasis, thin-section CT enables assessment of parenchymal fibrosis. Also, thin-section CT may assist in the evaluation of disease activity by means of accurate depiction of ground glass attenuation **(Terriff et al, 1992; Leung et al, 1993; Remy-Jardin et al, 1993c)**.

Owing to the accuracy of thin-section CT, so, what is the diagnostic benefit of spiral CT in evaluating infiltrative and/ or destructive lung changes. A few preliminary results suggest potential clinical applications of spiral CT of the lungs. Narrow collimation spiral CT and sliding thin-slab-maximum or-minimum intensity projection are the most promising developments.

Narrow collimation spiral scanning

Engeler et al. **(1994)** evaluated the accuracy of narrow collimation spiral scanning in the diagnosis of interstitial lung disease when four contiguous sections were acquired at three anatomical levels (the aortic arch, the carina, and 2 cm above the diaphragm). They concluded that the use of volumetric high-resolution CT increased the diagnostic accuracy, particularly in respect of bronchiectasis at lung base, without increasing the peak skin radiation exposure. With the availability of four contiguous scans per anatomical level, the subjective confidence in the interpretation and the number of motion- free studies are increased.

Maximum intensity projection (MIP)

Recent advances in CT have led to the introduction of volumetric scanning, which has the potential to combine the advantages of continuous data acquisition with the use of volume rendering techniques. At the level of a region of interest, a focal spiral CT acquisition is performed. From this data set, contiguous transverse CT scans are reconstructed then stacked to produce slabs of lung parenchyma. On each slab the maximum intensity projection algorithm is applied, enabling projection of the brightest voxels encountered along each ray, thus resulting in a MIP image **(Remy-Jardin et al, 1996a)**.

Detection of micronodules

Although thin-section CT is the most accurate technique for evaluation of diffuse infiltrative lung diseases, a few limitations of this CT technique have been reported with regard the detection of micronodular infiltration **(Remy-Jardin et al. 1990, 1991)**. On thin sections, micronodules may be difficult to distinguish from vessels seen on end (when equal in diameter to nearby vessels) and also from confluence of abnormal linear areas of attenuation.

In order to confirm or rule out radiographic suspicion of micronodular infiltration, Remy-Jardin et al **(1996a)** evaluated 81 patients suspected of having diffuse infiltrative lung disease. Each patient underwent both 8-mm and 1-mm conventional CT scans at the level of region of interest, completed by a focal spiral CT evaluation at the level of the region of interest. In this study group, the sensitivity of MIP was found to be significantly higher than that of conventional CT in detecting lung micronodules.

As the advantage of MIP over a single section is that vessels can be appreciated over a much longer segment of their course, the concurrent improvement in vessel and micronodule conspicuity accounted for the more frequent identification of centrilobular and perivascular changes on MIP images. However, care must be taken to differentiate actual perivascular micronodules from the beaded appearance of MIP artifacts due to partial volume averaging. These artifacts have been described as stair-step vessels and are expected to be found at the level of vessels that pass obliquely through the volume **(Napel 1995)**.

These preliminary results suggest that a combination of conventional CT and MIP should be employed to achieve an adequate evaluation of mild forms of micronodular lung infiltration. Since patients cannot be imaged with multiple CT techniques because of the high radiation dosage and time constraints, a focal spiral CT acquisition over a region of interest could complement the conventional CT study performed over the entire thorax.

Detection of bronchiectasis and peripheral mucoid impactions

Diagnosis of mucoid impaction in the peripheral bronchioles on thin-section CT scans is usually based on the identification of short and non tapering tubular areas of attenuation, seen as either single or branched structures **(Muller and Miller 1995)**. Two studies have evaluated the role of spiral CT in detecting peripheral bronchiectasis and mucoid impaction. Remy-Jardin et al **(1996a)** found that MIP enabled identification of a greater number of bronchiolar changes compared with 1-mm conventional CT scans. Also Engeler et al. **(1994)** observed that traction bronchiectasis could be accurately differentiated from vessels or small pulmonary nodules only by examination of four contiguous scans generated from volumetric CT acquisition.

Minimum intensity projection

The result of the minimum intensity projection (mIP) is to retain low-density structures at the expense of blood vessels. Consequently, this technique results in improved airway visibility along greater portions of their lengths and could detect mild forms of emphysema. Emphysema is a pathological diagnosis, which is diagnosed on the basis of combination of clinical, functional, and radiographic findings. Whereas radiographic assessment of emphysema requires moderate to severe destruction, it has been shown that CT is effective in the detection and quantification of emphysema **(Muller et al, 1988; Klein et al, 1992)**. However, several authors have pointed out that mild emphysema may be missed on CT scans and the severity of emphysema may be underestimated **(Miller et al, 1989)**. Evaluating 29 patients with no chest x-ray evidence of emphysema with conventional thin-section CT and mIP immediately before surgery, Remy-Jardin et al. **(1996b)** found that volumetric CT could complement the visual inspection of CT images for the recognition of emphysema. The subjective superiority of mIP is directly related to the suppression of highly attenuated structures, i.e., vessels and fissures, with subsequent uniform appearance of lung parenchyma.

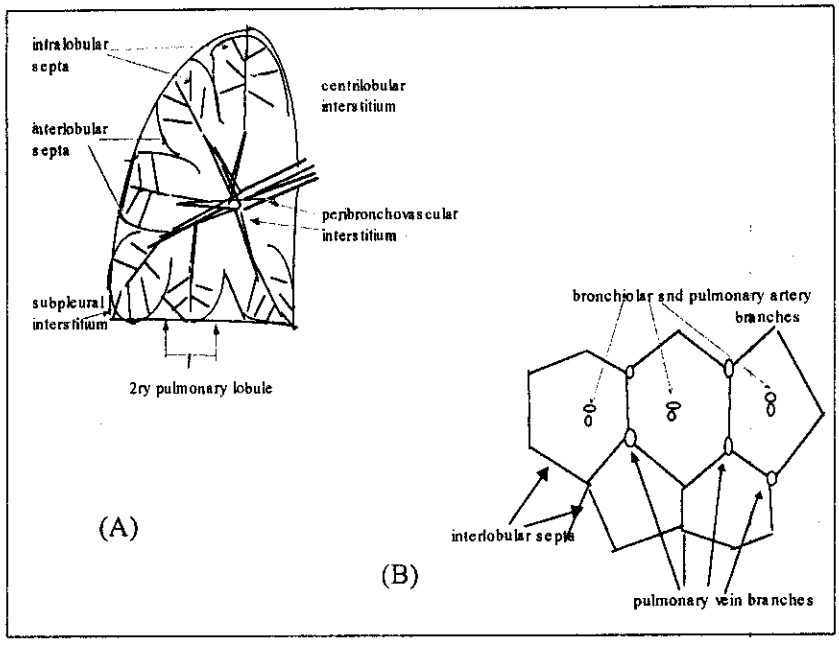

Fig.7

(A)Components of the lung interstitium. The peribronchovascular interstitium and centrilobular interstitium constitutes the axial fiber system. The subpleural interstitium and interlobular septa constitutes the peripheral fiber system. The intralobular interstitium is equivalent to the septal fibers.

(B)Pulmonary lobules are supplied by small bronchiolar and pulmonary artery branches, which are central in location, and are variably marginated by connective tissue interlobular septa that contain pulmonary vein and lymphatic branches.(After Webb et al, 1996)

NORMAL HRCT LUNG ANATOMY

The accurate interpretation of high-resolution CT (HRCT) images require a detailed understanding of normal lung anatomy and the pathologic alterations in normal lung anatomy that occur in the presence of diseases.

THE LUNG INTERSTITIUM

The lung is supported by a network of connective tissue fibers, called the lung interstitium. Although the lung interstitium is not generally visible on HRCT in normal subjects, interstitial thickening is often recognizable. The lung interstitium has several components **(Weibel, 1979) (fig 7a)**.

The *peribronchovascular interstitium* is a system of fibers that invests bronchi and pulmonary arteries. In the parahilar regions the peribronchovascular interstitium forms a strong connective tissue sheath that surrounds large bronchi and arteries. The more peripheral continuum of this interstitial fiber system, associated with small centrilobular bronchioles and arteries, is usually termed *centrilobular interstitium*, although the term *centrilobular peribronchovascular interstitium* would be appropriate. Taken together, the peribronchovascular interstitium and centrilobular interstitium correspond to the "axial fiber system "described by Weibel, which extends peripherally from pulmonary hila to the level of the alveolar ducts and sacs **(Weibel, 1979)**. The *subpleural interstitium*, is located beneath the visceral pleura, and envelops the lung in a fibrous sac from which connective tissue septa penetrate into the lung parenchyma. These septa include the *interlobular septa.* The subpleural interstitium and interlobular septa are both parts of the "peripheral fiber system "described by Weibel **(1979)**.

The *intralobular interstitium* is a network of thin fibers that forms a fine connective tissue mesh in the walls of alveoli, and thus bridges the gap between the centrilobular interstitium in the center of the lobules, and the interlobular septa and subpleural interstitium in the lobular periphery. Together, the intralobular

interstitium, peribronchovascular interstitium, centrilobular interstitium, subpleural interstitium, and interlobular septa form a continuous fiber skeleton for the lung. The intralobular interstitium corresponds to the septal fibers described by Weibel (1979).

Large bronchi and arteries

Within the lung parenchyma, the bronchi and pulmonary artery branches are closely associated and branch in parallel; they are encased by the peribronchovascular interstitium, which extends from the pulmonary hila into the peripheral lung. Since some lung diseases produce thickening of the peribronchovascular interstitium in the central or parahilar lung in relation to large bronchi and pulmonary vessels. When imaged at an angle to their longitudinal axis, central pulmonary arteries normally appear as rounded or elliptic opacities on HRCT, accompanied uniformly thin-walled bronchi of similar shape. When imaged along their axis, bronchi and vessels should appear roughly cylindrical, or show slight tapering as they branch, depending on the length of the segment that is visible; tapering of a vessel or bronchus is most easily seen when a long segment is visible.

The diameter of an artery and its neighboring bronchus should approximately equal, although vessels may appear slightly larger than their accompanying bronchus, particularly in dependent lung regions. Although the presence of bronchi larger than their adjacent arteries is often assumed to indicate bronchial dilatation, or bronchiectasis, bronchi may appear larger than adjacent arteries in a significant number of normal subject.

The outer walls of visible pulmonary artery branches form a smooth and sharply defined interface with the surrounding lung, whether they are seen in cross-section or along their length. The walls of large bronchi, outlined by lung on one side, and the air in the bronchial lumen on the other, should appear to be smooth and of uniform thickness. Thickening of the peribronchial and perivascular interstitium

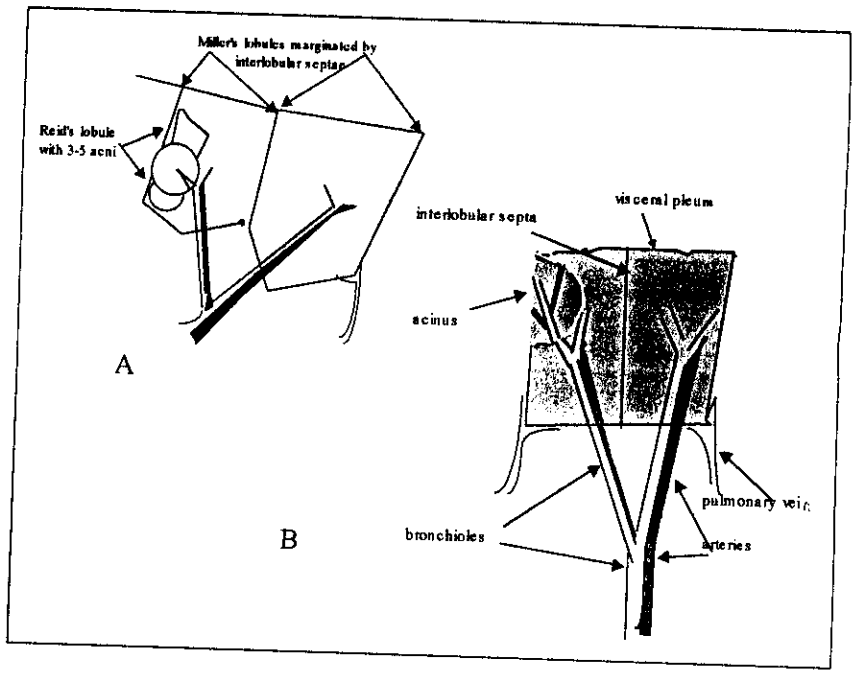

Fig.8

(A)Relative size and relationships of "Miller's lobule" and "Reid's lobule"

(B)Anatomy of the secondary pulmonary lobule, as defined by Miller. Two adjacent lobules are shown in the diagram. Lobules are marginated by thin interlobular septa containing pulmonary vein branches. Bronchioles and pulmonary arteries are centrilobular.(After Webb et al, 1996).

can result in irregularity of the interface between arteries and bronchi and the adjacent lung **(Zerhouni, 1989; Zerhouni et al, 1985)**.

The wall thickness of conducting bronchi and bronchioles is approximately proportional to their diameter, at least for bronchi distal to the segmental level. In general, the thickness of the wall of a bronchus or bronchiole less than 5-mm in diameter should measure from 1/6 to1/10 of its diameter **(Weibel & Taylor 1988)**. Because bronchi taper and become thinner walled as they branch, and thus become more difficult to see, as they become more peripheral. Bronchi less than 2 mm in diameter, and closer than 2 cm to the pleural surface are not normally visible on HRCT **(Webb et al, 1988; Murata et al, 1986)**.

The secondary pulmonary lobule

The secondary pulmonary lobule, as defined by Miller, refers to the smallest unit of lung structure marginated by connective tissue septa **(Weibel & Taylor 1988; Miller 1947)**. Secondary lobules are easily visible on the surface of the lung because of these septa **(Weibel & Taylor 1988; Heitzman et al, 1969)(fig 7b)**. The terms secondary pulmonary lobule, secondary lobule, and pulmonary lobule are often used interchangeably, and are used as synonymous. The term primary pulmonary lobule has also used by Miller to describe a much smaller lung unit associated with a single alveolar duct **(Heitzman et al, 1969; Miller 1947)**. Secondary pulmonary lobules are irregularly polyhedral in shape and somewhat variable in size, measuring approximately 1 to 2.5 cm in diameter in most locations **(Weibel 1979, Weibel & Taylor 1988)(fig 8b)**. Each secondary lobule is supplied by a small bronchiole and pulmonary artery, and is variably marginated by connective tissue interlobular septa that contain pulmonary vein and lymphatic branches **(Heitzman et al, 1969)**. Secondary pulmonary lobules are made up of a limited number of pulmonary acini, usually a dozen or fewer **(Weibel 1990)**. A pulmonary acinus is defined as the portion of the lung parenchyma distal to a terminal bronchiole and is supplied by a first order respiratory bronchiole **(Reid**

1958). Since respiratory bronchioles are the largest airways that have alveoli in their walls, an acinus is the largest lung unit in which all airways participate in gas exchange. Acini are usually described ranging from 6 to 10 mm in diameter **(Gamsu et al, 1971)**. Miller has defined the secondary lobule as the smallest lung unit marginated by connective tissue septa. Reid has suggested an alternate definition of the secondary pulmonary lobule, based on the branching pattern of peripheral bronchioles, rather than the presence and location of connective tissue septa **(Reid 1958)(fig 8a)**. On bronchograms, small bronchioles can be seen to arise at intervals of 5 to 10 mm from large airways, the so-called centimeter pattern of branching; these small bronchioles then show branching at approximately 2-mm intervals, the "millimeter pattern"**(Reid & Simon 1958)**. Airways showing the millimeter pattern of branching are considered by Reid to be intralobular, with each branch corresponding to a terminal bronchiole **(Reid 1958)**. Lobules are considered to be the lung units supplied by 3 to 5 "millimeter pattern"bronchioles. Although Reid's criteria delineate lung units of approximately equal size, about 1 cm in diameter and containing 3 to 5 acini, it should be noted, that this definition does not necessarily describe lung units equivalent to secondary lobules as defined by Miller and marginated by interlobular septa **(Itoh et al, 1993)**, although a small Miller's lobule can be the same as a Reid's lobule. Miller's definition is most applicable to the interpretation of HRCT, and is widely accepted by pathologists because interlobular septa are visible on histologic sections **(Itoh et al, 1993)**. The term secondary pulmonary lobule to refer to a lobule as defined by Miller.

Anatomy of the secondary lobule and its components.

HRCT can show many features of the secondary pulmonary lobule in both normal and abnormal lungs, and many lung diseases particularly interstitial diseases, produce some characteristic changes in lobular structures **(Webb, 1989)**. The visibility of normal lobular structures on HRCT is related to their size and orientation relative to the plane of scan, although size is most important. The

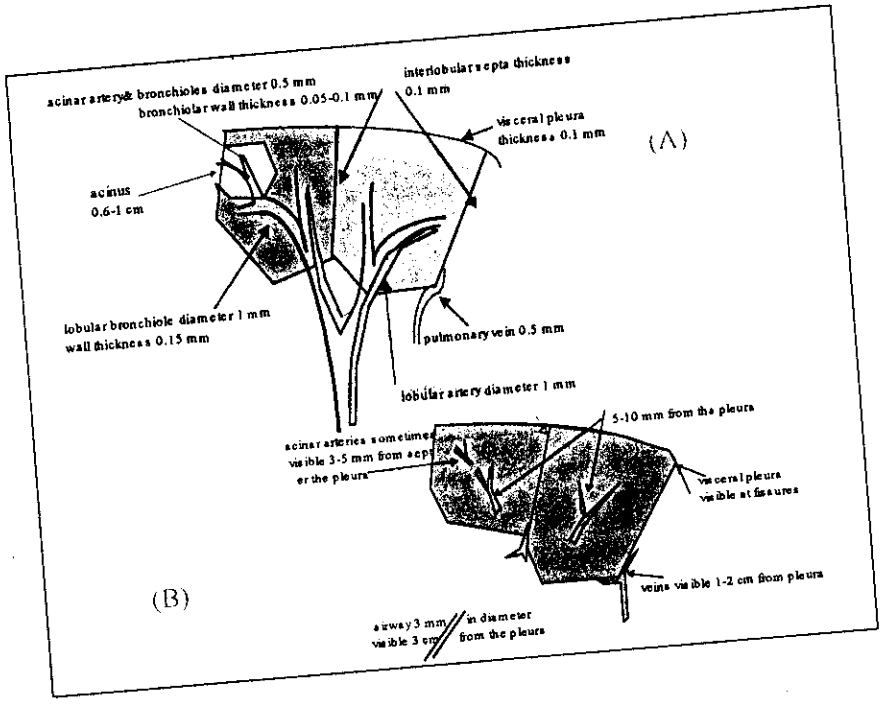

Fig.9

Dimensions of secondary lobular structure (A), and their visibility on HRCT (B).

(After Webb et al, 1996)

smallest structures visible on HRCT range from 0.3 to 0.5 mm in thickness; thinner structures, measuring 0.1 to 0.2 mm, are occasionally seen **(fig 9).**

For the purposes of the interpretation of HRCT, the secondary lobule is the most appropriately conceptualized as having three principal components:

1. The interlobular septa and contiguous subpleural interstitium,
2. The centrilobular or lobular core structures, and
3. The lobular parenchyma and acini.

1-Interlobular septa

Anatomically, secondary lobules are marginated by connective tissue interlobular septa, which extend inward from the pleural surface. These septa are part of the peripheral interstitial fiber system described by Weibel **(1979)**, that extends over the surface of the lung beneath the visceral pleura. Pulmonary vein and lymphatics lie within the connective tissue interlobular septa that marginate the lobule. The interlobular septa are thickest and most numerous in the apical, anterior, and lateral aspects of the upper lobes, the anterior and lateral aspects of the middle lobe and lingula, the anterior and diaphragmatic surfaces of the lower lobes, and along the mediastinal pleural surfaces **(Reid &Rubino 1959)**; thus, secondary lobules are best defined in these regions. Septa measure About 100 *um* (0.1 mm) in thickness in a subpleural location **(Webb 1989; Weibel 1979)**. Within the central lung, interlobular septa are thinner and less well defined than peripherally, and lobules are more difficult to identify in this location. Peripherally, interlobular septa measuring 100 *um* or 0.1 mm in thickness are at the lower limit of HRCT resolution **(Murata et al, 1986)**.

On clinical scans in normal patients, interlobular septa are less commonly seen. A few septa are often seen in the lung periphery in normal subjects, but they tend to be inconspicuous; normal septa are most often seen anteriorly and along the mediastinal pleural surfaces **(Zerhouni 1989; Aberle et al, 1988)**. When visible, they are usually seen extending to the pleural surface. In the central lung, septa are thinner than they are peripherally and are infrequently seen in normal subjects;

often interlobular septa that are clearly defined in this region are abnormally thickened.

2-The centrilobular region and lobular core structures

The central portion of the lobule, referred to as the centrilobular region or lobular core **(Heitzman et al, 1969)**, contains the pulmonary artery and bronchiolar branches that supply the lobule, as well as some supporting connective tissue (the centrilobular interstitium)**(Webb et al, 1988; Murata et al, 1986)**. The branching of the lobular bronchiole and artery are irregularly dichotomous **(Itoh et al, 1993)**. In other words, when they divide, they divide into two branches that are usually of different sizes; one branch is nearly the same size as the one it arose from, and the other is smaller. Thus, on bronchograms or arteriograms (or HRCT), there often appears to be a single dominant bronchiole and artery in the center of the lobule, which give off smaller branches at intervals along their length.

The HRCT appearances and visibility of structures in the lobular core are determined by their size. Secondary lobules are supplied by arteries and bronchioles measuring 1 mm in diameter, while intralobular terminal bronchioles and arteries measure about 0.7 mm in diameter, and acinar bronchioles and arteries range from 0.3 mm to 0.5 mm in diameter. Arteries of this size can be easily resolved using HRCT technique **(Webb et al, 1988; Murata et al, 1986)**.

On clinical scans, a linear, branching, or dot-like opacity seen within the center of a lobule, or within a centimeter of the pleural surface, represents the interlobular artery branch or its divisions **(Webb 1989)**. The smallest arteries resolved extend to within 3 to 5 mm of the pleural surface or lobular margin and are as small as 0.2 mm in diameter **(Webb et al, 1988)**.

Regarding the visibility of bronchioles in normals, it is necessary to consider bronchiolar wall thickness rather than bronchiolar diameter. For a 1-mm bronchiole supplying a secondary lobule, the thickness of its wall measures approximately 0.15 mm; this is at the lower limit of HRCT resolution. The wall of a terminal bronchiole measures only 0.1 mm in thickness, and that of an acinar

bronchiole only 0.05 mm, both of which are below the resolution of HRCT technique for tubular structure. In one in vitro study only bronchioles having a diameter of 2 mm or more or having a wall thickness of 0.1 mm were visible using HRCT **(Murata et al, 1986)**; and resolution is certainly less than this on clinical scans. On clinical HRCT, intralobular bronchioles are not normally visible, and bronchi or bronchioles are not normally seen within 2 cm of the pleural surface.

3-The lobular parenchyma

The substance of the secondary lobule, surrounding the lobular core and contained within the interlobular septa, consists of functioning lung parenchyma, namely alveoli and the associated pulmonary capillary bed, supplied by small airways and branches of the pulmonary arteries and veins. This parenchyma is supported by a connective tissue stroma; a fine network of very thin fibers within the alveolar septa called the ***intralobular interstitium*** **(Weibel 1979; Weibel & Taylor 1988)**, which are normally invisible. On HRCT, the lobular parenchyma should be of greater opacity than air, but this difference may vary with window settings. Some small intralobular vascular branches are often visible. All three interstitial fiber systems described by Weibel (axial, peripheral, and septal) are represented at the level of the pulmonary lobule, and abnormalities in any can produce recognizable lobular abnormalities on HRCT **(Webb et al, 1988)**.

The pulmonary acinus

Pulmonary acini are not normally visible on HRCT **(Itoh et al, 1993)**. As with lobules, acini vary in size. They are usually described as ranging from 6 to 10 mm in diameter **(Gamsu et al, 1971)**. Secondary pulmonary lobules defined by the presence of connective tissue interlobular septa usually consist of a dozen or fewer pulmonary acini **(Weibel, 1990).** First order respiratory bronchioles and the acinar artery branch measure about 0.5 mm in diameter; thus, intralobular acinar arteries are large enough to be seen on HRCT in some normal subjects **(Weibel & Taylor 1988)**. Murata et al **(1986)** have shown that pulmonary artery branches as small as 0.2 mm, associated with a respiratory bronchiole, and thus acinar in nature, are

visible on HRCT, and extend to within 3 to 5 mm of the lobular margins or pleural surface.

Lobular anatomy and the concept of "cortical" and "medullary"lung

Peripheral or cortical lung

Cortical lung can be conceived of as consisting of two or three rows of well-organized and well defined secondary pulmonary lobules, which together form a layer about 3 to 4 cm in thickness at the lung periphery and along lung surfaces adjacent to fissures **(Heitzman et al, 1969)**. The pulmonary lobules in the lung cortex are relatively large in size, and are marginated by interlobular septa that are thicker and better defined than in other parts of the lung; thus cortical lobules tend to be better defined than those in the central or medullary lung. Bronchi and pulmonary vessels in the lung cortex are relatively small.

Lobules in the lung cortex tend to be relatively uniform in appearance. They can appear cuboidal, or be shaped like a truncated cone or pyramid **(Heitzman et al, 1969)**. However, the size, shape, and appearance of pulmonary lobules on HRCT are significantly affected by the orientation of the scan plane relative to the central and longitudinal axes of the lobules.

Central or "medullary" lung

Pulmonary lobules in the central or medullary lung are smaller and more irregular in shape than in the cortical lung, and are marginated by interlobular septa that are thinner and less well defined. When visible, medullary lobules may appear hexagonal or polygonal in shape. In contrast with the peripheral lung, parahilar vessels and bronchi in the lung medulla are large and easily seen on HRCT.

The subpleural interstitium and visceral pleura

The visceral pleura consists of a single layer of flattened mesothelial cells, subtended by layers of fibroelastic connective tissue; it measures 0.1 to 0.2 mm in thickness **(Agostoni et al, 1969)**. The connective tissue component of the visceral pleura is generally referred to on HRCT as the *subpleural interstitium,* and is part of the "peripheral" interstitial fiber network described by Weibel **(1979)**. The

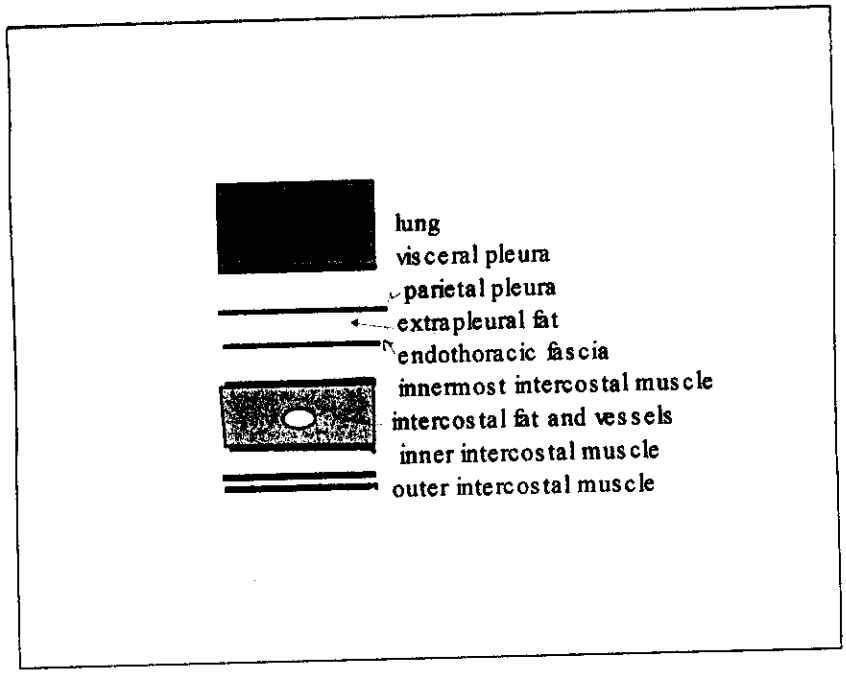

Fig.10

Anatomy of the pleural surface and chest wall (After Webb et al, 1996)

subpleural interstitium contains small vessels, which are involved in the formation of pleural fluid, and lymphatic branches. Interstitial lung diseases that affect the interlobular septa, or result in lung fibrosis, often result in abnormalities of the subpleural interstitium.

Abnormalities of the subpleural interstitium can be recognized over the costal surfaces of the lung, but are more easily seen in relation to the major fissures, where two layers of the visceral pleura and subpleural interstitium come in contact. In contrast to conventional CT, in which the obliquely oriented major fissures are usually seen as broad bands of increased or decreased opacity, these fissures are consistently visualized on HRCT as continuous, smooth, very thin, linear opacities. Normal fissures are less than 1-mm thick, smooth in contour, uniform in thickness, and sharply defined. The visceral pleura and subpleural interstitium along the costal surfaces of lung are not visible on HRCT in normal subjects.

The parietal pleura

The parietal pleura, as with the visceral pleura, consists of a mesothelial cell membrane in association with a thin layer of connective tissue. The parietal pleura is thinner than the visceral pleura, measuring about 0.1 mm (**Agostoni et al, 1969**). External to the parietal pleura is a thin layer of loose areolar connective tissue or extrapleural fat, which separates the pleura from the fibroelastic endothoracic fascia and lines the thoracic cavity. External to the endothoracic fascia are the innermost intercostal muscles pass between adjacent ribs, but do not extend into the paravertebral regions (**fig 10**).

A window level /width settings of 50/350 HU are best for evaluating the parietal pleura and adjacent chest wall. Images at level of -600, with an extended window width of 2000 are also useful in evaluating the relationship of peripheral parenchymal abnormalities to the pleural surfaces (**Murata et al, 1989**).

On HRCT in normal patients, the innermost intercostal muscles are often visible as 1- to 2-mm thick stripes (the intercostal stripes) of soft tissue opacity at the

Normal expiratory HRCT

The lung parenchyma normally increases in CT attenuation as lung volume is reduced during expiration. This change can generally be recognized on HRCT as an increase in lung opacity **(Verschakelen et al, 1993)**. In a study **(Webb et al, 1993)** of ten normal subjects using dynamic expiratory HRCT, an increase in lung attenuation averaging 200 HU was consistently seen during expiration, but the increase was variable, and ranged from 84 to 372 HU. In some normal subjects, small areas of focal lucency are visible on expiratory scans; in these regions, lung does not increase normally in attenuation, probably as a result of focal air trapping. This appearance is most typical in the superior segments of the lower lobes, or in the anterior middle lobe or lingula **(Webb et al, 1993)**.

Changes in lung attenuation during expiration can be related to changes in cross-sectional lung area as shown on HRCT. Simply stated, cross-sectional lung area decreases during expiration at the same time attenuation increases. Normal morphologic changes that can be seen on expiratory CT also include a decrease in tracheal diameter associated with the anterior bowing of the tracheal membrane **(Stern et al, 1993)**, and a small decrease in the diameter of the bronchi.

Pulmonary vessels may appear somewhat to increase in diameter on expiration. Following expiration, dependent lung regions increase more in attenuation than do nondependent lung regions. This results in an accentuation of the normal anterior to posterior lung attenuation gradient **(Webb et al, 1993)**.

HRCT FINDINGS OF DIFFUSE LUNG DISEASE

Generally, HRCT findings of lung disease can be classified into four large categories based on their appearances. These are (i) increased lung opacity, (ii) linear and reticular opacities, (iii) decreased lung opacity, and (iv) nodules and nodular opacities (**fig 11**).

I-INCREASED LUNG OPACITY

Increased lung opacity, or parenchymal opacification, is a common finding on HRCT in patients with chronic lung disease. Increased lung opacity is generally described as being *ground-glass opacity* or *consolidation* (**Webb et al, 1993a**).

"Ground-Glass" opacity

Ground-glass opacity is a nonspecific term referring to the presence on HRCT of a hazy increase in lung opacity that is not associated with obscuration of underlying vessels; if vessels are obscured, the term *consolidation* is generally used (**Webb et al, 1993a**). This finding can reflect the presence of a number of diseases, and can be seen in patients with minimal air-space disease, interstitial thickening, or both (**Leung et al, 1993**).

Ground-glass opacity results from the volume averaging of morphologic abnormalities below the resolution of HRCT (**Remy-Jardin et al, 1993d**). It can reflect the presence of minimal thickening of the "septal" or alveolar interstitium, thickening of alveolar walls, or the presence of cells or fluid partially filling the alveolar spaces. Ground-glass opacity has been seen in patients with histologic findings of mild or early interstitial inflammation or infiltration (**Leung et al, 1993**). Also, when a small amount of fluid is present within the alveoli, as can occur in the early stages of an air-space filling disease, the fluid tends to layer against the alveolar walls, and is indistinguishable on HRCT from alveolar wall thickening (**Naidich et al, 1985**). In a study comparing the results of lung biopsy

with HRCT in 22 patients who showed ground-glass opacity, 14% had diseases primarily affecting air-spaces, 32% had a mixed interstitial and air-space abnormality, and 54% had a primarily interstitial abnormality **(Leung et al, 1993)**. Ground-glass opacity is difficult to recognize if it is of minimal severity and is diffuse in distribution, involving all lung regions to an equal degree. However, this abnormality is usually patchy in distribution, affecting some lung regions while others appear spared; this "geographic" appearance of the lung parenchyma makes it easier to detect and diagnose with confidence. In some patients, entire lobules may appear abnormally dense, while adjacent lobules appear normal **(Webb 1989; Naidich et al, 1985)**. Ground-glass opacity can involve individual segments, lobes, or can involve nonsegmental regions of the lung. The presence of air-filled bronchi that appear "too black" within an area of lung can also be clue as to the presence of ground-glass opacity; this "dark bronchus" appearance is essentially that of an air-bronchogram.

Significance and Differential Diagnosis of Ground-Glass opacity

Ground-glass opacity is a highly significant finding, as it often indicates the presence of an active and potentially treatable process. Of the 22 patients with ground-glass opacity studied by Leung et al. **(1993)**, 18(82%) were considered to have active or potentially reversible disease on lung biopsy. Because of its association with active lung disease, the presence of ground-glass opacity often leads to further diagnostic evaluation, including lung biopsy, depending on the clinical status of the patient. Also, when a lung biopsy is performed, areas of ground-glass opacity can be targeted by the surgeon or bronchoscopist. Since such areas are most likely to be active, they are most likely to yield diagnostic material. Because ground-glass opacity can reflect the presence of either fibrosis or inflammation, one should be careful to diagnose an active process only when ground-glass opacity is unassociated with HRCT findings of fibrosis, or is the predominant finding. If ground-glass opacity is only seen in lung regions also showing significant HRCT findings of fibrosis, such as traction bronchiectsis or

honeycombing, it is most likely that fibrosis will be the predominant histologic abnormality. For example, in a study by Remy-Jardin et al. **(1993c)**, patients showing traction bronchiectasis or bronchiolectasis on HRCT in regions of ground-glass opacity all had fibrosis on lung biopsy. On the other hand, in patients without traction bronchiectasis in areas of ground-glass opacity, 92% were found to have active inflammatory disease on lung biopsy.

A large number of diseases can be associated with ground-glass opacity on HRCT **(Table 1)**. In many, this reflects the presence of similar histologic reactions in the early or active stages of disease, with inflammatory exudates involving the alveolar septa and alveolar spaces, although this pattern can be the result of a variety of pathologic processes. The most common causes of ground-glass opacity include usual interstitial pneumonia (UIP) or desquamative interstitial pneumonia (DIP) associated with idiopathic pulmonary fibrosis or scleroderma, bronchiolitis obliterans organizing pneumonia, sarcoidosis, and hypersensitivity pneumonitis. Other diseases associated with this finding include pneumonia particularly *pneumocystis carinii* pneumonia, alveolar proteinosis, acute interstitial pneumonia or other causes of diffuse alveolar damage or the adult respiratory distress syndrome (ARDS), pulmonary edema of various causes, pulmonary hemorrhage, respiratory bronchiolitis, and early radiation pneumonitis **(Remy-Jardin et al, 1993c; Bessis et al, 1992; Godwin et al, 1988; Ikezoe et al, 1990)**.

In patients with UIP or DIP associated with idiopathic pulmonary fibrosis, scleroderma, or other collagen vascular diseases, a number of studies have correlated the presence of ground-glass opacity on HRCT with biopsy results, response to treatment, and patient survival **(Remy-Jardin et al, 1993c; Lee et al, 1992)**. In histologic studies of patients with interstitial pneumonia, ground-glass opacity has been shown to be associated with the presence of alveolar wall or intra-alveolar inflammation. In patients with UIP, ground-glass opacity is associated with alveolar septal inflammation, varying numbers of intra-alveolar histiocytes, and varying degrees of fibrosis; ground-glass opacity in patients with

DIP largely reflects the presence of macrophages within the alveoli (**Leung et al, 1993; Wells et al, 1992**).

Table (1): Differential diagnosis of ground-glass opacity (Webb et al, 1996)

Diagnosis	Comments
1. Usual interstitial pneumonia(UIP)	• Often present; patchy; usually dominant in peripheral, posterior, and basal regions; finding of fibrosis often present; consolidation less common
2. Desquamative interstitial pneumonia(DIP)	• Always present; diffuse or patchy; usually dominant in basal, peripheral regions; findings of fibrosis less common than in UIP; consolidation much less common
3. Lymphocytic interstitial pneumonia(LIP)	• Diffuse, patchy, or centrilobular
4. Bronchiolitis obliterans organizing pneumonia/ cryptogenic organizing pneumonia(BOOP/COP)	• Common, consolidation may also present; can be dominant in peripheral regions; can be nodular
5. Sarcoidosis	• Present in about 25%; patchy; nodules usually predominate; consolidation less common
6. Hypersensitivity pneumonitis	• Very common; patchy or nodular; can be centrilobular; consolidation less common
7. Alveolar proteinosis	• Very common; patchy or diffuse; septal thickening common; fibrosis rare; consolidation much less common
8. Acute interstitial pneumonia	• Always present; consolidation common; patchy or diffuse
9. Pneumocystis carinii pneumonia, CMV pneumonia	• Common; diffuse or patchy; consolidation can be present; septal thickening in subacute stage
10. Eosinophilic pneumonia	• Sometimes seen; consolidation more common
11. Respiratory bronchiolitis	• Common, patchy or nodular; can be centrilobular; consolidation not reported
12. Pulmonary edema	• Diffuse or centrilobular; septal thickening
13. Pulmonary hemorrhage	• Patchy or focal

Technical Considerations and Pitfalls in the Diagnosis of Ground-Glass Opacity

First, it is important to recognize that since ground-glass opacity reflects the volume averaging of morphologic abnormalities below the resolution HRCT, the thicker the collimation used for scanning, the more likely volume averaging will occur, regardless of the nature of the anatomic abnormality. Thus, ground-glass opacity should be diagnosed only on scans obtained with thin collimation.

The diagnosis of ground-glass opacity is largely subjective and based on a qualitative assessment of lung attenuation. The use of lung attenuation measurements to determine the presence of increased lung density in patients with ground-glass opacity is difficult because of the variations in attenuation measurements that are known to be associated with gravitational density gradients in the lung, the level of inspiration, and fluctuations that occur as a result of patient size, position, chest wall thickness, and kVp. Using consistent window settings for the interpretation of HRCT is very important. Using too low a window mean in conjunction with a relatively narrow window width can give the appearance of a diffuse ground-glass abnormality **(Remy-Jardin et al, 1993d)**. In assessing the attenuation of the lung parenchyma, it is often helpful to compare its appearance to that of air in the trachea or bronchi; if tracheal air appears gray instead of black, then increased attenuation or "grayness" of the lung parenchyma may not be significant.

Also, increased lung opacity is commonly seen in dependent lung on HRCT, largely as a result of volume loss in the dependent lung parenchyma; so-called dependent density **(Aberle et al, 1988)**. This can result in a stripe of ground-glass opacity several centimeters thick in the posterior lung of supine patients; prone scans allow this transient finding to be distinguished from a true abnormality. Similarly, on expiration, because of a reduction of the amount of air within alveoli, lung regions increase in attenuation and can mimic the appearance of ground-glass opacity resulting from lung disease.

Furthermore, in patients who have emphysema or other causes of lung hyperlucency such as airways obstruction and air trapping, normal lung regions can appear relatively dense, thus mimicking the appearance of ground-glass opacity. This pitfall can usually be avoided if consistent window settings are used for interpretation of scans. The use of expiratory HRCT can also be of value in distinguishing the presence of heterogeneous lung attenuation resulting from emphysema or air trapping from that representing ground-glass opacity **(Webb et al, 1996)**.

Consolidation

Increased lung attenuation with obscuration of underlying pulmonary vessels; air-bronchograms may be present **(Webb et al, 1993; Tuddenham 1984)**. HRCT has little to add to the diagnosis of patients with clear-cut evidence of consolidation visible on chest radiographs. However, HRCT can allow the detection of consolidation before it becomes diagnosable radiographically.

By definition, diseases that produce consolidation, are characterized by a replacement of alveolar air by fluid, cells, tissue, or material **(Naidich et al, 1985)**. Most are associated with air-space filling, but diseases that produce extensive, confluent interstitial abnormalities, such as UIP or sarcoidosis, can also result in this finding **(Leung et al, 1993)**. Air-space nodules or focal areas of ground-glass opacity are often seen in association with areas of frank consolidation. The differential diagnosis of consolidation includes pneumonia of different causes including *pneumocystis carinii* pneumonia, bronchiolitis obliterans organizing pneumonia, hypersensitivity pneumonitis, Eosinophilic pneumonia, radiation pneumonitis, bronchioloalveolar carcinoma and lymphoma, UIP, alveolar proteinosis, acute interstitial pneumonia, sarcoidosis, drug reaction, pulmonary edema and ARDS **(Naidich et al, 1985; Godwin et al, 1988; Leung et al, 1993; Ikezoe et al, 1990; Muller et al, 1990)**. Lobar consolidation is often due to infection, although consolidation due to alveolar proteinosis can also have a lobar predominance. Chronic lung diseases that result in consolidation often involve the

lung in a patchy fashion. Patchy consolidation can show a nonanatomic and nonsegmental distribution, but can also be panlobular, involving individual lobules, or can appear nodular and centrilobular on HRCT **(Webb 1989; Naidich et al, 1985)**.

1I-LINEAR AND RETICULAR OPACITIES

Thickening of the interstitial fiber network of the lung by fluid, fibrous tissue or because of interstitial infiltration by cells or other material, primarily results in an increase in linear or reticular lung opacities as seen on HRCT. Linear or reticular opacities can be manifested by the interface sign, peribronchovascular interstitial thickening, interlobular septal thickening, intralobular interstitial thickening, honeycombing, subpleural lines, centrilobular or lobular core abnormalities, and airway abnormalities.

The interface sign

The presence of irregular interfaces between the aerated lung parenchyma and bronchi, vessels, or the visceral pleural surfaces, has been termed the *interface sign* by Zerhouni et al. **(Zerhouni 1989; Zerhouni et al, 1985)**

The interface sign is commonly seen in patients with an interstitial abnormality, regardless of its cause. In the original description of the interface sign, this finding was visible in 89% of patients with interstitial lung disease **(Zerhouni et al, 1985)**. The interface sign is generally associated with an increase in lung reticulation; the presence of thin linear opacities contacting the bronchi, vessels, or pleural surfaces is responsible for their having an irregular or spiculated appearance on HRCT. These linear opacities generally represent thickened interlobular septa or thickened intralobular interstitial fibers.

Peribronchovascular Interstitial Thickening

Central bronchi and pulmonary arteries are surrounded by a strong connective tissue sheath, termed the *peribronchovascular interstitium*, that extends from the level of the pulmonary hila into the peripheral lung, in relation to alveolar ducts

and alveoli; this is termed the *axial interstitium* by **Weibel (1979)**. Thickening of the parahilar peribronchovascular interstitium occurs in many diseases that cause a generalized interstitial abnormality **(Webb 1989)**. Peribronchovascular interstitial thickening is common in patients with lymangitic spread of carcinoma **(Johkoh et al, 1992)** or interstitial pulmonary edema, and can be seen in many diseases that result in pulmonary fibrosis, particularly sarcoidosis, which has a propensity to involve the peribronchovascular interstitium. Peribronchovascular interstitial thickening has been also reported in as many as 19% of patients with chronic hypersensitivity pneumonitis **(Adler et al, 1992)**.

Since the thickened peribronchovascular interstitium cannot be distinguished from the underlying opacity of the bronchial wall or pulmonary artery, this abnormality is usually perceived on HRCT as (i) an increase of the bronchial wall thickness and (ii) an increase in diameter of pulmonary artery branches **(Munk et al, 1988)**. Apparent bronchial wall thickening is the easiest of these two findings to recognize, and is exactly equivalent to "peribronchial cuffing" seen on plain chest radiographs in patients with an interstitial abnormality. Thickening of peribronchovascular interstitium can appear smooth, nodular, or irregular in different diseases.

Smooth peribronchovascular interstitial thickening is most typical of patients with lymphangitic spread of carcinoma and interstitial pulmonary edema **(Bessis et al, 1992)**, but can be seen in patients with fibrotic lung disease as well. Nodular thickening of the peribronchovascular interstitium is particularly common in sarcoidosis and lymphangitic spread of carcinoma. The presence of irregular peribronchovascular interstitial thickening, as an example of the interface sign, is most frequently seen in patients with peribronchovascular and adjacent lung fibrosis. Extensive peribronchovascular fibrosis can result in the presence of large conglomerate masses of fibrous tissue. This can occur in patients with sarcoidosis, silicosis, tuberculosis, and talcosis.

Peribronchovascular interstitial thickening is easy to diagnose if it is of a marked degree, and bronchial walls appear several millimeters in thickness, or bronchovascular structures show evidence of the interface sign or nodules. However, the diagnosis of minimal peribronchovascular thickening can be difficult and quite subjective, particularly if the abnormality is diffuse and symmetric. Although the thickness of the wall of a normal bronchus should measure from 1/6 to 1/10 of its diameter **(Weibel & Taylor 1988)**, there are no reliable criteria as to what represents the upper limit of normal for the combined thickness of bronchial wall and the surrounding interstitium. Furthermore, these measurements vary depending on the lung window chosen, and too low a window mean can make normal bronchi or vessels appear abnormal. Fortunately, however, in many patients with peribronchovascular interstitial thickening, and particularly in patients with lymphangitic spread of carcinoma and sarcoidosis, this abnormality is unilateral or patchy, sparing some areas of the lung. In such patients, normal and abnormal lung regions can be easily contrasted. As a rule, bronchial walls in corresponding regions of one or both lungs should be quite similar in thickness.

In patients with lung fibrosis and peribronchovascular interstitial thickening, bronchial dilatation is commonly present, resulting from traction by fibrous tissue on the bronchial walls. This is termed *traction bronchiectasis*; it typically results in irregular bronchial dilatation that appears "varicose"**(Webb et al, 1988)**. Traction bronchiectasis usually involves the segmental and subsegmental bronchi, and is most commonly visible in the parahilar regions in patients with significant lung fibrosis. It can also affect small peripheral bronchi or bronchioles; an occurrence termed *traction bronchiolectasis.*

Bronchial wall thickening, which occurs in patients with true bronchiectasis, produces an abnormality that closely mimics the HRCT appearance of peribronchovascular interstitial thickening. However, airway diseases and interstitial diseases can usually distinguished on the basis of symptoms or

pulmonary function abnormalities, and confusion between these two is not often a problem in clinical diagnosis. In addition, some HRCT findings also allow these two entities to be distinguished. First, peribronchovascular interstitial thickening is often associated with other findings of interstitial disease, such as septal thickening, honeycombing, or the interface sign, while bronchiectasis usually is not. Second, in patients with bronchiectasis, the abnormal thick-walled and dilated bronchi often appear much larger than the adjacent pulmonary artery branches. This results in the appearance of large ring shadows, each associated with a small, rounded opacity, a finding that has been termed the *signet-ring sign,* and is considered to be diagnostic of bronchiectasis **(Naidich et al, 1982; Grenier et al, 1986; Grenier et al, 1990)**. In patients with peribronchovascular interstitial thickening, on the other hand, the size relationship between the bronchus and artery is maintained, and they appear of approximately equal size.

Interlobular Septal Thickening

Thickening of the interlobular septa is commonly seen in patients with interstitial lung disease. On HRCT, numerous clearly visible interlobular septa almost always indicate the presence of an interstitial abnormality; only a few septa are visible in normal patients. Septal thickening can be seen in the presence of interstitial fluid, cellular infiltration, or fibrosis.

Within the peripheral lung, thickened septa 1 to 2 cm in length may outline part of, or an entire lobule, are usually seen extending to the pleural surface, being roughly perpendicular to the pleura **(Webb 1989; Aberle et al, 1988a)**. Lobules at the pleural surface may have a variety of appearances, but are often longer than they are wide, resembling a cone or truncated cone. Within the central lung, thickened septa outline lobules that are 1 to 2.5 cm in diameter, and appear polygonal, or sometimes hexagonal, in shape. Lobules delineated by thickened septa commonly contain a visible dot-like or branching centrilobular pulmonary artery.

Thickened interlobular septa also have been described using the terms "septal lines", "peripheral lines", "short lines", and "interlobular lines "**(Aberle et al,**

1988; Akira et al, 1990). Thickened septa outlining one or more pulmonary lobules have been described as producing a" large reticular pattern"**(Zerhouni 1989)** or "polygons", and, if they can be seen contacting the pleural surface, as "peripheral arcades "or "polygonal arcades"**(Stein et al, 1987)**.

Septal thickening can be smooth, nodular, or irregular in contour in different pathologic processes.

Smooth septal thickening is seen in patients with pulmonary edema **(Cassart et al, 1993)**, lymphangitic spread of carcinoma or lymphoma **(Munk et al, 1988)**, alveolar proteinosis **(Godwin et al, 1988)**, interstitial infiltration associated with amyloidosis **(Graham et al, 1992)**, in some patients with pneumonia, and in a small percentage of patients with pulmonary fibrosis. Nodular or beaded septal thickening occurs in lymphangitic spread of carcinoma or lymphoma **(Stein et al, 1987)**, sarcoidosis, silicosis or coal worker's pneumoconiosis **(Remy-Jardin et al, 1990a)**. and amyloidosis **(Graham et al, 1992)**. In patients who have interstitial fibrosis, septal thickening visible on HRCT is often irregular in appearance **(Webb et al, 1988)**.

Although interlobular septal thickening can be seen on HRCT in association with fibrosis and honeycombing, is not usually a predominant feature **(Nishimura et al, 1992)**. Generally speaking, in the presence of significant fibrosis and honeycombing, distortion of lung architecture make the recognition of thickened septa difficult. Among patients with pulmonary fibrosis and end-stage lung disease, the presence of interlobular septal thickening on HRCT is most frequent in patients with sarcoidosis (present in 56% of patients), and is relatively uncommon in those with usual interstitial pneumonia (UIP) of various causes, asbestosis, and hypersensitivity pneumonitis **(Primack et al, 1993)**.

The frequency of septal thickening and fibrosis in patients with sarcoidosis reflects the tendency of active sarcoid granulomas to involve the interlobular septa. In patients with idiopathic pulmonary fibrosis or UIP of other cause, the appearance of irregular septal thickening correlates with the presence of fibrosis

predominately affecting the periphery of the secondary lobule (**Nishimura et al, 1992**).

Parenchymal Bands

The term *parenchymal bands* has been used to describe non-tapering, reticular opacities, from 2 to 5 cm in length, that can be seen in patients with pulmonary fibrosis or other causes of interstitial thickening (**Aberle et al, 1988**). They are often peripheral and generally contact the pleural surface. In some patients, these bands represent contiguous thickened interlobular septa, have the same significance and differential diagnosis as septal thickening (**Akira et al, 1990**). Parenchymal bands visible on HRCT can also represent areas of peribronchovascular fibrosis, coarse scars, or atelectasis associated with lung or pleural fibrosis (**Akira et al, 1990**). These non-septal bands are often several millimeters thick, irregular in contour, and associated with significant distortion of the adjacent lung parenchyma and bronchovascular structures (**Im et al, 1993**). Parenchymal bands have been reported as most common in patients with asbestos-related lung and pleural disease, sarcoidosis with interstitial fibrosis, silicosis associated with progressive massive fibrosis and conglomerate masses, and tuberculosis. In patients with asbestos exposure, multiple parenchymal bands are common; in one study (**Aberle et al, 1988**) multiple parenchymal bands were seen in 66% of asbestos-exposed patients. These bands can reflect thickened interlobular septa, indicating pulmonary fibrosis, or areas of atelectasis and focal scarring occurring in association with pleural plaques (**Aberle et al, 1988**).

Subpleural Interstitial Thickening

Usually, thickening of the interlobular septa within the peripheral lung is associated with thickening of the "subpleural interstitium"(**Webb 1989**); both the septa and the subpleural interstitium are part of the "peripheral" interstitial fiber system described by **Weibel (1979)**. Subpleural interstitial thickening can be difficult to recognize in locations where the lung contacts the chest wall or

mediastinum, but is easy to see adjacent to the major fissures. Since two layers of the subpleural interstitium are seen adjacent to each other in this location, any subpleural abnormality appears twice as "abnormal" as it does elsewhere. Thus "thickening of the fissure" can represent subpleural interstitial thickening. If the thickening is smooth, it may be difficult to distinguish from fissural fluid. If the interface sign is present, and the thickening is irregular **(Zerhouni 1989)**, or if the thickening is nodular, an interstitial abnormality is more easily diagnosed.
Subpleural interstitial thickening is more common than septal thickening in patients with idiopathic pulmonary fibrosis (IPF) or usual interstitial pneumonia of any cause. The presence of subpleural interstitial fibrosis with irregular or "rugged" pleural surfaces has been reported by Nishimura et al. **(1992)** as a common finding in IPF, correlating with the presence of fibrosis predominately affecting the lobular periphery; this finding was present in 94% of cases of IPF he studied. A subpleural predominance of fibrosis can also be seen in patients with collagen vascular diseases and drug reactions **(Colby 1993)**.
Remy-Jardin et al. **(1990)** have reported the appearance of subpleural micronodules, defined as less than 7 mm in diameter, on HRCT in patients with sarcoidosis, coal worker's pneumoconiosis, lymphangitic spread of carcinoma, and in a small percentage of normal subjects.

Intralobular Interstitial Thickening

Thickening of the intralobular interstitium results in a fine reticular pattern as seen on HRCT, with the lines of opacity separated by a few millimeters. Lung regions showing this finding characteristically have a fine mesh or net-like appearance. Intralobular bronchioles are often visible on HRCT in patients with intralobular interstitial thickening and fibrosis because of a combination of their dilatation "traction bronchiolectasis" and thickening of peribronchiolar interstitium which surrounds them. Interlobular septal thickening may or may not be present in patients with intralobular interstitial thickening; when thickened septa are visible, they appear irregular. The pleural surface also appears irregular in the presence of

intralobular interstitial thickening. Intralobular interstitial thickening can also be described using the term *intralobular lines* **(Webb et al, 1988)**. This finding has also been called the *small reticular pattern* **(Zerhouni et al, 1985)**.

Intralobular interstitial thickening as perceived on HRCT reflects thickening of the distal peribronchovascular interstitial tissues, in relation to small arteries and bronchioles, or thickening of the intralobular interstitium. It is most commonly seen in patients with pulmonary fibrosis. In patients with idiopathic pulmonary fibrosis (IPF) or other causes of usual interstitial pneumonia (UIP), such as rheumatoid arthritis, scleroderma, or other collagen vascular diseases, fibrosis tends to predominately involve alveoli in the periphery of acini, resulting in a "peripheral acinar distribution" of interstitial fibrosis **(Colby 1993)**; this histologic finding correlates with the presence of intralobular lines on HRCT. In addition, the HRCT pattern of intralobular interstitial thickening can reflect the presence of very small honeycomb cysts or dilated bronchioles associated with surrounding lung fibrosis.

Intralobular interstitial thickening can also be seen in the absence of significant fibrosis, in patients with lymphangitic spread of carcinoma, pulmonary edema, and alveolar proteinosis **(Munk et al, 1988)**.

Subpleural lines

A curvilinear opacity a few millimeters thick, less than 1 cm from the pleural surface, and paralleling the pleura, was first described in patients with asbestosis **(Yoshimura et al, 1986)**. It has been reported that a subpleural curvilinear shadow, or subpleural line, is much more common in patients with asbestosis than those with idiopathic pulmonary fibrosis of other causes of UIP. Indeed, the presence of a subpleural line in nondependent lung has been reported in 41% of patients with clinical findings of asbestosis **(Aberle et al, 1988)**. The presence of subpleural line also has been reported as common in patients with scleroderma who have interstitial disease **(Swensen et al, 1992)**.

It was originally suggested that a subpleural line reflects the presence of fibrosis associated with honeycombing **(Yoshimura et al, 1986)**, and in some patients, a confluence of honeycomb cysts can result in somewhat irregular subpleural line. However, the appearance of a subpleural line has been reported to occur as a result of the confluence of peribronchiolar interstitial abnormalities in patients with asbestosis, representing early fibrosis with associated alveolar flattening and collapse **(Akira et al, 1990)**. In these patients honeycombing was not present. A subpleural line can be seen in normal patients as a result of atelectasis within the dependent lung (e.g., the posterior lung when the patient is positioned supine) **(Morimoto et al, 1989)**. Also, a thicker, less well-defined subpleural opacity, a so-called dependent density **(Aberle et al, 1988)**, can be seen in normal subjects as a result of volume loss. Such normal posterior lines and opacities are transient, and disappear in the prone position.

Centrilobular (Lobular core) Abnormalities

Centrilobular linear or reticular abnormalities can reflect interstitial thickening or bronchiolar abnormalities such as bronchiolar dilatation and the finding of "tree-in-bud."

Interstitial thickening

Diseases that cause interstitial thickening often result in prominence of the centrilobular vessel, which normally appears as a dot, Y-shaped, or X-shaped branching opacity. This finding represents an abnormality of the intralobular component of the peribronchovascular interstitium, termed the *centrilobular interstitium.* It is exactly analogous to the peribronchovascular interstitial thickening in the parahilar lung **(Aberle et al, 1988)**. On HRCT, a linear, branching, or dot-like abnormality may be seen. Thickening of the intralobular bronchovascular interstitium is usually associated with interlobular septal thickening or intralobular interstitial thickening, but sometimes occurs as an isolated abnormality. Centrilobular interstitial thickening is common in patients

with lymphangitic spread of carcinoma or lymphoma (**Munk et al, 1988**), and interstitial pulmonary edema (**Todo & Herman, 1986**). In patients with lung fibrosis, centrilobular interstitial thickening is common but almost always associated with honeycombing or intralobular lines.

Bronchiolar Dilatation and "Tree-in-Bud "

The intralobular bronchiole, which is not seen in normal subjects, is sometimes visible on HRCT in patients with centrilobular interstitial thickening because of a combination of (i) increased attenuation of surrounding lung, (ii) Thickening of the peribronchiolar interstitium, and (iii) dilatation of the bronchiole, which occurs as a result of fibrosis.

Diseases that involve small airways can result in increased prominence of centrilobular branching structures recognizable as an increase in reticulation on HRCT (**Akira et al, 1988**). Visibility of the centrilobular bronchiole in the absence of other findings of interstitial thickening should suggest airways disease; this finding can indicate dilatation of the bronchiole and bronchiolar wall thickening, or peribronchiolar fibrosis or inflammation. In some patients, small airways that are dilated and/or filled with pus, mucus, or inflammatory exudate appear as small, well-defined, centrilobular nodular, linear, or branching structures of soft-tissue opacity (**Gruden et al, 1994**). This appearance on HRCT has been likened to a *tree-in-bud* (**Im et al, 1993**).

Abnormal bronchioles producing a tree-in-bud appearance can be usually distinguished from normal centrilobular vessels by their more irregular appearance, a lack of tapering, or bulbous appearance at the tips of small branches. This latter appearance reflects the presence of bronchiolar dilatation or peribronchiolar inflammation. Centrilobular bronchiolar abnormalities characterized by dilatation and tree-in-bud are seen in patients with Asian panbronchiolitis (**Akira et al, 1988**), endobronchial spread of TB (**Im et al, 1993**) or nontuberculous mycobacteria, cystic fibrosis, and bronchopneumonia, bronchiectasis of any cause. In patients with Asian panbronchiolitis, prominent

branching centrilobular opacities represent dilated bronchioles with inflammatory bronchiolar wall thickening and abundant intraluminal secretions **(Akira et al, 1993)**. Similarly, in patients with active TB, a tree-in-bud appearance was visible in 72% of patients in one study **(Im et al, 1993)**, correlating with the presence of solid caseous material within terminal and respiratory bronchioles.

III-DECREASED LUNG OPACITY AND CYSTIC ABNORMALITIES

A variety of abnormalities result in decreased lung attenuation or air-filled cystic lesions on HRCT. These include honeycombing, bronchiectasis, emphysema, lung cysts, cavitary nodules, mosaic perfusion, and air trapping due to airways disease. In most of cases these can be readily distinguished on the basis of HRCT findings **(Hogg 1991)**.

Honeycombing

Extensive interstitial and alveolar fibrosis that results in alveolar disruption and bronchiolectasis produces the classic and characteristic appearance of *honeycombing or honeycomb lung*. Pathologically, honeycombing is defined by the presence of small air-containing cystic spaces, generally lined by bronchiolar epithelium, having thickened walls composed of dense fibrous tissue. Honeycombing indicates the presence of end-stage lung and can be seen in almost any process leading to end-stage pulmonary fibrosis **(Primack et al, 1993)**. These cysts have fibrous walls and are lined by bronchiolar epithelium. On HRCT, honeycombing is characterized by the presence of air-filled, cystic spaces several millimeters to several centimeters in diameter, which often predominate in a peripheral and subpleural location, occur in several layers, and are characterized by clearly definable walls, 1 to 3 mm in thickness **(Webb et al, 1988)**. In contradistinction to the lung cysts seen in patients with lymphangiomyomatosis and histiocytosis X, and the lucencies seen in patients with centrilobular

emphysema, honeycomb cysts tend to share walls. The presence of honeycombing on HRCT indicates the presence of severe fibrosis.

Large subpleural cystic spaces, several centimeters in diameter, can be associated with honeycombing, mimicking the appearance of bullae. These large cysts tend to predominate in the upper lobes. These large honeycomb cysts decrease in size on expiratory scans **(Aquino et al, 1994)**; this change would not be expected of bullae. Subpleural honeycomb cysts typically occur in several contiguous layers; this finding can allow honeycombing to be distinguished from subpleural emphysema (paraseptal emphysema) since subpleural cysts usually occur in a single layer **(Webb et al, 1996).**

Lung Cysts

On HRCT, the term *lung cyst* is used to refer to a thin-walled (usually>3 mm), well-defined and circumscribed, air-containing lesion **(Naidich 1991)**. Lung cysts are also defined as having a wall composed of one of a variety of cellular elements, usually fibrous or epithelial in nature **(Tuddenham 1984)**. For example, in patients with end-stage pulmonary fibrosis, honeycomb cysts are lined by bronchiolar epithelium; on the other hand, in patients with lymphangiomyomatosis the cysts are lined by abnormal spindle cells resembling smooth muscle. Lymphangiomyomatosis (LAM) and histiocytosis X often produce multiple lung cysts, whose appearance on HRCT is usually quite distinct from that of honeycombing **(Moore et al, 1989; Muller et al, 1990b)**. The cysts have a thin wall, ranging up to a few millimeters in thickness, associated findings of fibrosis are usually absent or much less conspicuous than they are in patients with honeycombing and end-stage lung disease. In LAM and histiocytosis X, the cysts are usually interspersed within areas of normal-appearing lung.

In patients with histiocytosis X, the cysts can have bizarre shapes because of the fusion of several cysts or perhaps because they represent ectatic and thick-walled bronchi. Although confluent cysts can also be seen with LAM, they are less

common; in patients with LAM, cysts generally appear rounder, and more uniform in size, than those seen with histiocytosis X.
Lung cysts should be distinguished from air-containing spaces such as emphysematous bullae, blebs, and pneumoatoceles **(Webb et al, 1996)**.

Emphysema

Emphysema is defined as a permanent, abnormal enlargement of airspaces distal to the terminal bronchiole, accompanied by destruction of the walls of the involved airspaces **(Naidich 1991)**, Emphysema can be accurately diagnosed using HRCT, and results in focal areas of very low attenuation that can be easily contrasted with surrounding, higher attenuation, normal lung parenchyma if sufficiently low window means (-600 HU to -800 HU) are used. Although some types of emphysema can have walls visible on HRCT, these are usually inconspicuous **(Muller et al, 1988, Miller et al, 1989)**.
In many patients it is possible to classify the type of emphysema on the basis of HRCT appearance **(Webb et al, 1988)**. *Centrilobular (centriacinar) emphysema,* is characterized on HRCT by the presence of multiple small lucencies that predominate in the upper lobes. Even if the centrilobular location of these lucencies is not visible, a spotty distribution is typical of centrilobular emphysema. In most cases, the areas of low attenuation seen on HRCT in patients with centrilobular emphysema lack a visible wall, although very thin walls are occasionally visible. In severe cases, the areas of centrilobular emphysema become confluent. *Panlobular (panacinar) emphysema* typically results in an overall decrease in lung attenuation, and a reduction in size of pulmonary vessels, without the focal areas of lucency typically seen in patients with centrilobular emphysema. Areas of panlobular emphysema typically lack visible walls. This form of emphysema has been described as a diffuse simplification of lung architecture. Severe centrilobular emphysema can mimic this appearance. *Paraseptal (distal acinar) emphysema* results in the presence of subpleural

lucencies, which often sharp very thin walls that are visible on HRCT; paraseptal emphysema can be seen as an isolated abnormality, but is often associated with centrilobular emphysema. *Irregular air-space enlargement*, previously known as irregular or cicatricial emphysema, can be seen in association with fibrosis, as in silicosis and progressive massive fibrosis **(Kinsella et al, 1990)**. The appearance of panlobular emphysema and centrilobular emphysema can mimic the presence of honeycombing or lung cysts in some patients.

Paraseptal emphysema vs. Honeycombing

In patients with paraseptal emphysema, areas of lung destruction are typically marginated by thin linear opacities, visible on HRCT, that extend to the pleural surface. These linear opacities often correspond to interlobular septa and sometimes are associated with minimal fibrosis. Because they are subpleural and marginated by visible walls, areas of paraseptal emphysema can resemble the appearance of honeycombing. Honeycomb cysts are usually smaller, usually occur in several layers, tend to predominate at the lung bases, are associated with disruption of lobular architecture and other findings of fibrosis. On the other hand, areas of paraseptal emphysema are often larger and associated with bullae, usually occur in a single layer, predominate in the upper lobes, and may be associated with other findings of emphysema, but are typically unassociated with significant fibrosis **(Webb et al, 1996)**.

Cavitary Nodules

Cavitary nodules have thicker and more irregular walls than do lung cysts, but there is some overlap between these appearances. Such nodules have been reported in histiocytosis X, tuberculosis, fungal infection, and sarcoidosis, but could also be seen in patients with rheumatoid lung disease, septic embolism, pneumonia, metastatic tumor, Wegener's granulomatosis, etc. Also some nodular opacities having central lucencies, may represent dilated bronchioles surrounded

by areas of consolidation or interstitial thickening **(Moore et al, 1989; Im et al, 1993; Nishimura et al, 1993)**.

Bronchiectasis

Bronchiectasis is generally defined as localized, irregular bronchial dilatation **(Grenier et al, 1993)**. While bronchiectasis usually results from chronic infection, airway obstruction by tumor, stricture, impacted material, or inherited abnormalities can also play a significant role. Bronchiectasis has also been classified into three types, depending on the morphology of the abnormal bronchi, although these distinctions are of little clinical value **(Naidich 1991)**.

Cylindrical bronchiectasis, the mildest form of this disease, is characterized on HRCT by the presence of thick-walled bronchi, which extend into the lung periphery and fail to show normal tapering. On HRCT, bronchi are not normally visible in the peripheral 2 cm of lung, but in patients with bronchiectasis, bronchial wall thickening, peribronchial fibrosis, and dilatation of bronchial lumen, allow them to be seen in the lung periphery. Depending on their orientation relative to the scan plane they can simulate "tram tracks" or can show the "signet-ring sign," in which dilated, thick-walled bronchus and its accompanying pulmonary artery branch are seen adjacent to each other **(Naidich et al, 1982)**. Ectatic bronchi containing fluid or mucus appear as tubular opacities.

Varicose bronchiectasis is similar in appearance to cylindrical bronchiectasis; however, with varicose bronchiectasis the bronchial walls are more irregular, and can assume a beaded appearance. The term *string of pearls* has been used to describe varicose bronchiectasis. Traction bronchiectasis often appears varicose.

Cystic bronchiectasis most often appears as a group or cluster of air-filled cysts, but cysts can also be fluid-filled, giving the appearance of a" cluster of grapes." Cystic bronchiectasis is often patchy in distribution, allowing it to be distinguished from a cystic lung disease such as LAM. Also, air-fluid levels, which may be

present in the dependent portions of the cystic dilated bronchi, are a very specific sign of bronchiectasis, and are not usually seen in patients with lung cysts.

Traction Bronchiectasis

In patients with lung fibrosis and distortion of the lung architecture, traction bronchiectasis is commonly present. Traction by fibrous tissue on the walls of the bronchi results in irregular bronchial dilatation, or bronchiectasis, which is typically "varicose" in appearance **(Webb et al, 1988)**.

Traction bronchiectasis usually involves the segmental and subsegmental bronchi, can also affect small peripheral bronchi or bronchioles. Dilatation of the intralobular bronchioles because of the surrounding fibrosis is termed *traction bronchiolectasis*. In patients with honeycombing, bronchial dilatation contributes to the cystic appearance seen on HRCT **(Nishimura et al, 1992)**.

The increased transpulmonary pressure and elastic recoil associated with advanced pulmonary fibrosis, along with local distortion of airways by fibrotic tissue, all contribute to the varicose dilatation of airways seen in these condition. Traction bronchiectasis is usually most marked in areas of lung that show the most severe fibrosis. It is commonly seen in association with honeycombing **(Webb et al 1996)**.

Use of Expiratory CT to Differentiate Mosaic Perfusion from Ground-Glass Opacity

Inhomogeneous lung attenuation visible on inspiratory scans can be the result of (i) ground-glass opacity, (ii) mosaic perfusion resulting from airways obstruction and reflex vasoconstriction, or (iii) mosaic perfusion resulting from vascular obstruction. In many patients with mosaic perfusion, HRCT findings of decreased vascular caliber in lucent lung regions, or airway abnormalities can be diagnostic; however, in others, HRCT findings are nonspecific.

Expiratory scans can usually allow the differentiation of patients with ground-glass opacity from those with mosaic perfusion resulting from airways obstruction. In patients with ground-glass opacity, expiratory HRCT typically shows a proportional increase in attenuation in areas of both increased and decreased opacity. In patients with mosaic perfusion resulting from airways disease, attenuation differences are accentuated on expiration; relatively dense areas increase in attenuation, while lower attenuation regions remains lucent. In patients with mosaic perfusion resulting from vascular disease, expiratory HRCT findings mimic those seen in patients with ground-glass opacity; both low-attenuation and high-attenuation regions increase in opacity **(webb et al, 1996)**.

IV-NODULES AND NODULAR OPACITIES

An approach to the assessment and differential diagnosis of multiple nodular opacities is based on a consideration of their size (small or large), distribution, and appearance (well-defined or ill-defined).

Small Nodules

The term *small nodule* is defined as a rounded opacity less than 1 cm in diameter, whereas *large nodule* is 1 cm or greater in diameter. Some authors have used *micronodule* to describe nodules that are either less than 3 mm **(Grenier et al, 1991)** or less than 7 mm in diameter **(Remy-Jardin et al, 1991)**, but it is not clear that this distinction is of value in differential diagnosis **(Grenier et al, 1991)**. Differences in the appearances of nodules that are predominantly "interstitial" or predominantly "air-space" in origin have been emphasized by several authors. Nodules considered to be interstitial are usually well defined despite their small size. Nodules as small as 1 to 2 mm in diameter can be detected on HRCT in patients with interstitial diseases such as sarcoidosis **(Murata et al, 1989)**, histiocytosis X **(Moore et al, 1989)**, silicosis and coal worker's pneumoconiosis **(Bergin et al, 1986)**, miliary TB **(Lee et al, 1993)**, and metastatic tumor **(Murata et al, 1992)**. Interstitial nodules usually appear to be of soft tissue attenuation and

obscure the edges of vessels or other structures in which they touch **(Akira et al, 1991)**. Air-space nodules are more likely to be ill defined; they can be of homogeneous soft-tissue attenuation, thus obscuring vessels, or hazy and less dense than adjacent vessels (so-called ground-glass opacity). A cluster or rosette of small nodules can also be seen **(Naidich et al, 1985)**. Air-space nodules have also been termed "acinar nodules, "because they approximate the size of acini, but these nodules are not truly acinar histologically, but tend to be centrilobular and peribronchiolar **(Itoh et al, 1978)**; *ill-defined nodule or air-space nodule* are preferable terms. Despite these differences in appearance, a distinction between interstitial and air-space nodules on the basis of HRCT findings can be quite difficult, because many nodular diseases affect both the interstitial and alveolar compartments histologically. The distribution or location of small nodules is more valuable in differential diagnosis than their appearance. In different conditions, small nodules can appear randomly distributed, perilymphatic in distribution, or predominantly centrilobular.

Random Distribution

Small nodules that appear randomly distributed in relation to structures of the secondary lobule are often seen in patients with miliary TB and miliary fungal infections **(Lee et al, 1993).** The nodules can be seen in relation to small vessels, interlobular septa, and the pleural surfaces, but do not appear to have a consistent or predominant relationship to any of these. In miliary TB or fungal infections, the nodules tend to be well defined and up to several millimeters in diameter. Hematogeneous metastases have a recognized tendency to predominate in the lung periphery and at the lung bases. As with miliary TB, the nodules can be seen in relation to small vessels in some locations, a fact, which likely reflects their mode of dissemination. In a study correlating HRCT and pathologic findings, nodules less than 3 mm in diameter had no consistent relationship to lobular structures. Nodules resulting from hematogeneous metastasis are characteristically well-defined **(Murata et al, 1992)**.

Perilymphatic Distribution

Nodules that predominate in relation to the parahilar peribronchovascular interstitium, the centrilobular interstitium, interlobular septa, and in a subpleural location are typical of patients with sarcoidosis, silicosis and coal worker's pneumoconiosis, and lymphangitic spread of carcinoma **(Colby, 1993).** This pattern of abnormalities has been termed lymphatic or perilymphatic, in that it corresponds to the distribution of lymphatics in the lung **(Remy-Jardin et al, 1990a).**

In nearly all patients with sarcoidosis, HRCT shows nodules, ranging in size from several millimeters to 1 cm or more in diameter **(Muller et al, 1989).** The nodules often appear sharply defined despite their small size. Nodules are most frequently seen in relation to the parahilar peribronchovascular interstitium, the subpleural interstitium, and small vessels; histologically small clusters of granulomas are visible in these locations **(Muller et al, 1989).** An upper lobe predominance of nodules is common in sarcoidosis **(Remy-Jardin et al, 1990).** Nodules can cavitate in only 3% of cases **(Grenier et al, 1991).**

Silicosis and coal worker's pneumoconiosis are associated with the presence of small nodules, usually measuring from 2 to 5 mm in diameter, which predominantly appear centrilobular and subpleural in location on HRCT **(Remy-Jardin et al, 1990).** These correlate with areas of fibrosis surrounding centrilobular respiratory bronchioles and involving the subpleural interstitium, and are caused by the accumulation of particulate material in these regions. In patients with silicosis, the nodules can calcify.

A few small subpleural and centrilobular nodules can also be seen in smokers probably related to the presence of fibrosis and accumulated particulate material in the peribronchiolar regions and at the bases of interlobular septa, and probably related to pathways of lymphatic drainage. Lymphocytic interstitial pneumonia (LIP) can result in the presence of lymphocytic and plasma cell infiltrates in

relation to the peribronchovascular interstitium, interlobular septa and centrilobular regions. On HRCT, ill-defined centrilobular opacities can be seen. Subpleural nodules have been reported in about 80% of patients with silicosis or coal worker's pneumoconiosis, 50% of patients with sarcoidosis, and are also common with lymphangitic spread of carcinoma **(Remy-Jardin et al, 1990)**. Confluent subpleural nodules can result in the appearance of "psudoplaques"; linear areas of subpleural opacity several millimeters in thickness that mimic the appearance of asbestos-related parietopleural plaques **(Remy-Jardin et al, 1990)**.

Centrilobular Distribution

Nodules limited to the centrilobular regions may be dense and of homogeneous opacity, or of ground-glass opacity, and range from a few millimeters to a centimeter in size. Either a single centrilobular nodule or a centrilobular rosette of nodules may be visible **(Naidich et al, 1985)**. Because of similar size of the secondary lobules, centrilobular nodules often appear to be evenly spaced. Centrilobular nodules are usually separated from the interlobular septa and pleural surfaces by a distance of several millimeters; in the lung periphery the nodules are usually centered 5 to 10 mm from the pleural surface. They do not usually occur in relation to interlobular septa or the pleural surfaces, as do random or perilymphatic nodules, and the subpleural lung is typically spared.

It is typical for centrilobular nodules to appear perivascular on HRCT, surrounding or obscuring the smallest pulmonary arteries visible on HRCT. On occasional cases, the air-filled centrilobular bronchiole can be recognized as a rounded lucency within a centrilobular nodule.

Centrilobular nodules can be seen in patients with a variety of diseases that primarily affect centrilobular bronchioles or arteries and result in inflammation or fibrosis of the surrounding interstitium and alveoli **(Colby 1993)**. Bronchiolar diseases most frequently result in this finding, sometimes in association with centrilobular airway dilatation or the appearance of a tree-in-bud. Well-defined,

small peribronchiolar nodules, representing interstitial granulomas, have been described in patients with histiocytosis X **(Moore et al, 1989)**. Ill-defined centrilobular opacities can occur in patients with endobronchial spread of TB or nontuberculous mycobacteria, lobular or bronchopneumonia **(Itoh et al, 1978)**, Asian panbronchiolitis **(Akira et al, 1988)**, hypersensitivity pneumonitis **(Lee et al, 1991)**, bronchiolitis obliterans with organizing pneumonia (BOOP)**(Muller et al, 1990)**, and respiratory bronchiolitis in smokers. bronchiolitis obliterans, bronchiectasis with surrounding fibrosis in cigarette smokers, asbestosis, pulmonary edema, vasculitis, and talcosis. Bronchioloalveolar carcinoma and endobronchial spread of tracheobronchial papillomatosis can also result in small centrilobular nodules **(Gruden & Webb 1993; Leung et al, 1993)**.

Large nodules

The term *large nodule* is used to refer to rounded opacities that are 1 cm or more in diameter. The term *mass* is generally used to describe nodular lesions that are greater than 3 cm in diameter **(Tuddenham 1984)**. Large nodules can be associated with a variety interstitial or air-space diseases, including those described above. In addition, in patients with diffuse or chronic lung disease, these can represent conglomerate masses of smaller nodules as are common in sarcoidosis or silicosis, infectious or inflammatory lesions, tumor nodules, infarctions, nodules of Wegener's granulomatosis **(Weir et al, 1992)**.

Conglomerate Nodules or Masses

In patients with disease characterized by small nodules, conglomeration or confluence of nodules can result in large nodular or mass-like opacities. Grenier et al. **(1991)** reported the presence of confluent nodules greater than 1 cm in 53% of patients with sarcoidosis. These masses were seen in upper lobes and peribronchovascular regions. These masses are often irregular in shape, surround the central bronchi and vessels, and can show small discrete nodules in their periphery.

Large masses of fibrous tissue may surround and encompass bronchi and vessels within the central or parahilar lung in patients with progressive fibrotic lung disease. The bronchi within these masses may be crowded together, reflecting the volume loss which is present, and are dilated as a result of fibrosis and traction bronchiectasis. Similar upper lobe masses associated with bronchiectasis have been reported in patients with TB, and are most frequent after treatment **(Im et al, 1993)**.

Patients with silicosis and coal workers who have complicated pneumoconiosis or progressive massive fibrosis, also show conglomerate masses in the upper lobes, but these are more typically of homogeneous opacity, and tend to be unassociated with visible traction bronchiectasis as seen in sarcoidosis. Also, areas of emphysema peripheral to the conglomerate masses are common **(Remy-Jardin et al, 1990a)**.

Focal fibrotic masses that are irregular in shape have been described as occurring in the peripheral lung, in relation to pleural abnormalities in patients with asbestos exposure. These represent focal areas of scarring or rounded atelectasis. It most always occurs in association with pleural disease, and typically contacts the pleural surface. Rounded atelectasis occurs most commonly in the posterior lung, in the paravertebral regions, and may bilateral. Bending or bowing of adjacent bronchi and arteries toward the area of atelectasis, because of volume loss or folding of lung is characteristic. This appearance has been likened to a "comet-tail." Air bronchograms within the mass can sometimes be seen **(Weir et al, 1992; Padley et al, 1993)**.